

# CONFORMALLY SYMMETRIC TRIANGULAR LATTICES AND DISCRETE $\vartheta$ -CONFORMAL MAPS

ULRIKE BÜCKING

**ABSTRACT.** Two immersed triangulations in the plane with the same combinatorics are considered as preimage and image of a discrete immersion  $F$ . We compare the cross-ratios  $Q$  and  $q$  of corresponding pairs of adjacent triangles in the two triangulations. If for every pair the arguments of these cross-ratios (i.e. intersection angles of circumcircles) agree,  $F$  is a discrete conformal map based on circle patterns. Similarly, if for every pair the absolute values of the corresponding cross-ratios  $Q$  and  $q$  (i.e. length cross-ratios) agree, the two triangulations are discretely conformally equivalent. We introduce a new notion, discrete  $\vartheta$ -conformal maps, which interpolates between these two known definitions of discrete conformality for planar triangulations. We prove that there exists an associated variational principle. In particular, discrete  $\vartheta$ -conformal maps are unique maximizers of a locally defined concave functional  $\mathcal{F}_\vartheta$  in suitable variables. Furthermore, we study conformally symmetric triangular lattices which contain examples of discrete  $\vartheta$ -conformal maps.

## 1. INTRODUCTION

Conformal maps of planar domains, that is, holomorphic maps with non-vanishing derivatives, build an important and classical subject in complex analysis which has been intensively studied. Conformality of a map  $f$  may be characterized by the fact that it infinitesimally preserves cross-ratios. In particular,  $f$  also preserves intersection angles and orientation. Moreover, the standard metric  $g$  of the complex plane is changed conformally by  $f$  to  $\tilde{g}$ , that is  $\tilde{g} = e^u g$  for some smooth function  $u$ . Note that all these properties are invariant under Möbius transformations.

In the last decades, a growing interest in discrete conformal maps has emerged. Thurston first introduced in [40] planar circle packings, that is configurations of touching discs corresponding to a triangulation, as discrete conformal maps. This idea has been extended to circle patterns which allow intersecting circles with fixed intersection angles, for instance Schramm's orthogonal circle patterns [34]. Many explicit classes of examples of circle packings or circle patterns which correspond to special conformal maps like polynomials, exponential functions,  $z^\gamma$ ,  $\log$ ,  $\operatorname{erf}$ , see [2, 34, 3, 1, 4, 5, 6], have been discovered using integrable structures or other additional properties. Furthermore, circle patterns (and circle packings) can be obtained from variational principles for the radii of the circles, see [18, 32, 9, 27]. Moreover, two circle patterns with the same underlying combinatorics may be considered as discrete conformal map if all intersection angles of corresponding pairs of circles for incident vertices agree, see for example [34, 27, 11].

Another more recent metric approach led to a different notion of discrete conformal maps based on discretely conformally equivalent triangulations [8, 13]. This notion was introduced by Luo in [30]. Here, the length cross-ratios (i.e absolute values of the cross-ratios) agree for corresponding pairs of incident triangles. For these discrete conformal maps there is only one explicit class of examples known so far, which corresponds to

exponential functions, see [41]. Nevertheless, conformally equivalent triangulations may also be obtained from a variational principle for the edge lengths, see [39, 7]. Moreover, there is a relation of this functional studied in [7] to a variational principle for circle patterns based on edge lengths. Note that there also exists a variational principle for more general discrete conformal changes of triangulations from a metric viewpoint, see [23].

In this article, we propose a new definition of discrete conformal maps  $F : T \rightarrow \widehat{T}$  between two immersed planar triangulations  $T$  and  $\widehat{T}$  with the same combinatorics which generalizes the two known notions based on circle patterns and discrete conformal equivalence. Recall that the cross-ratio of the four vertices of two incident triangles encode the intersection angle of the corresponding circumcircles of the triangles as well as the length cross-ratio. We may add circumcircles to all triangles of the triangulations  $T$  and  $\widehat{T}$ . In this way we obtain two *circle patterns* with the same combinatorics. Now  $F$  is discrete conformal if all intersection angles of these circumcircles agree for corresponding pairs of adjacent triangles. In terms of cross-ratios, this means that the arguments of the cross-ratios are the same for all pairs of adjacent triangles. Similarly, focusing on the absolute values of the cross-ratios of all corresponding pairs of adjacent triangles, we could call  $F$  discrete conformal if all length cross-ratios are preserved. Discrete  $\vartheta$ -conformality generalize these two notions of discrete conformality by including them into the one parameter family of definitions which interpolates smoothly between them. Instead of intersections angles or length cross-ratios, we preserve a combination of these values for an arbitrary, but fixed parameter  $\vartheta$ . See Section 2 for more details. Figure 1 shows some examples. There is also a relation to discrete holomorphic quadratic differentials defined by Lam and Pinkall in [29], see Subsection 4.2.

One main result of this paper is the proof in Section 5 that the condition for discrete  $\vartheta$ -conformal maps, see (3), is variational which is known to hold for circle patterns [9] and conformally equivalent triangulations [7]. This means that using suitable coordinates, discrete  $\vartheta$ -conformal maps correspond (locally) to critical points of a functional. Calculating the second derivative, we see the particularly nice property that the functional is concave and the Hessian is related to the cotan-Laplacian similarly as in the case of circle patterns and conformally equivalent triangulations. Thus convex optimization may be applied for obtaining critical points. Convexity also shows that the solutions are unique (up to a similarity transformation). Therefore, in appropriate coordinates, the triangulations corresponding to discrete  $\vartheta$ -conformal maps are locally rigid. It remains an open question to determine an explicit formula for this functional.

Our considerations in this article are motivated by a class of examples for discrete  $\vartheta$ -conformal maps, namely, conformally symmetric triangular lattices, see Section 4.1. These can be considered as discrete exponential functions or discrete Airy functions. We characterize and study this class of examples in Section 3.

Note that there exist several other approaches for discrete conformal maps. The earliest investigations resulted in the linear theory of discrete holomorphic maps, which also arises as suitable linearization of the (nonlinear) notions mentioned above, see for example [6, 10, 12]. Further studies of this approach can for example be found in [20, 22]. Apart from applications in numerics [17, 35, 19], this linear theory has been used for a rigorous study of dimers and the  $2D$ -Ising model in the context of probability, see [26, 36, 15, 16].

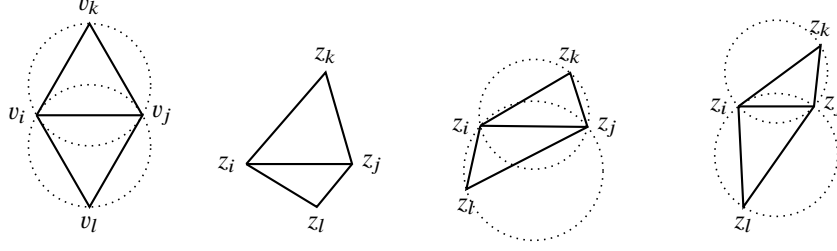


**Figure 1.** Examples of discrete  $\vartheta$ -conformal functions for two incident triangles (from left to right): original configuration of two equilateral triangles,  $\vartheta = 0$  (discrete conformal equivalence),  $\vartheta = \pi/2$  (circle pattern),  $\vartheta = \pi/3$  (new notion)

## 2. DEFINITIONS AND BASIC PROPERTIES

In any discrete setting, the domain of a smooth conformal map is replaced by a suitable discrete object. In the following, let  $T$  denote a (locally) embedded non-degenerate triangulation in the plane. Denote the vertices and edges of  $T$  by  $V$  and  $E$  respectively. Edges will often be written as  $e = [v_i, v_j] \in E$ , where  $v_i, v_j \in V$  are its incident vertices. For triangular faces we use the notation  $\Delta[v_i, v_j, v_k]$  enumerating the incident vertices with respect to the (counterclockwise) orientation of  $\mathbb{C}$ .

As a starting point for discrete conformal maps on  $T$ , we consider mappings  $F : T \rightarrow \mathbb{C}$  which are continuous, piecewise affine-linear on every triangle, and orientation preserving. For every interior vertex, all its adjacent triangles build a *flower*.  $F$  is called a *discrete immersion* if for every flower all pairs of image triangles only intersect in their common vertex or edge, so the image flower is embedded. The immersed image triangulation will be denoted by  $\widehat{T} = F(T)$  with vertices  $\widehat{V} = F(V)$  and edges  $\widehat{E} = F(E)$ . Given such a discrete immersion, when should it be called discrete conformal? In this article, we focus on the fact, that a smooth conformal map infinitesimally preserves cross-ratios. For the two triangulations  $T$  and  $\widehat{T}$  we can compute the cross-ratios of adjacent triangles in  $T$  and  $\widehat{T}$ , respectively. We will use the following definition of the *cross-ratio of four points*  $z_1, z_2, z_3, z_4 \in \mathbb{C}$ :

$$\text{cr}(z_1, z_2, z_3, z_4) = \frac{(z_1 - z_2)(z_3 - z_4)}{(z_2 - z_3)(z_4 - z_1)}.$$

For every interior edge  $[v_i, v_j]$  in  $T$  with adjacent triangles  $\Delta[v_i, v_j, v_k]$  and  $\Delta[v_i, v_l, v_j]$  as in Figure 2(c), we define

$$Q([v_i, v_j]) := \text{cr}(v_i, v_l, v_j, v_k), \quad (1)$$

$$q([v_i, v_j]) := \text{cr}(z_i, z_l, z_j, z_k), \quad (2)$$

where  $z_m = F(v_m)$  for  $m \in \{i, j, k, l\}$ . These cross-ratios are related to the geometric configuration of two incident triangles as  $q([v_i, v_j]) = |q([v_i, v_j])|e^{i\varphi}$ , where  $|q([v_i, v_j])| = |\text{cr}(z_i, z_l, z_j, z_k)|$  is also called *length cross-ratio* and  $\varphi \in (0, \pi)$  is the interior intersection angle of the two circumcircles of the triangles  $\Delta[z_i, z_l, z_j]$  and  $\Delta[z_i, z_j, z_k]$  in  $\widehat{T}$ . Note that for two embedded, non-degenerate, counterclockwise oriented triangles the logarithm of  $q$  (and analogously  $\log Q$ ) is well defined with values in  $\mathbb{R} + i(0, \pi)$  by taking  $\log(q([v_i, v_j])) := \log \frac{z_1 - z_2}{z_3 - z_2} + \log \frac{z_3 - z_4}{z_1 - z_4}$ . Furthermore, the values of  $q$  characterize the image triangulation  $\widehat{T}$  up to Möbius transformations, see also Lemma 2.2 below.

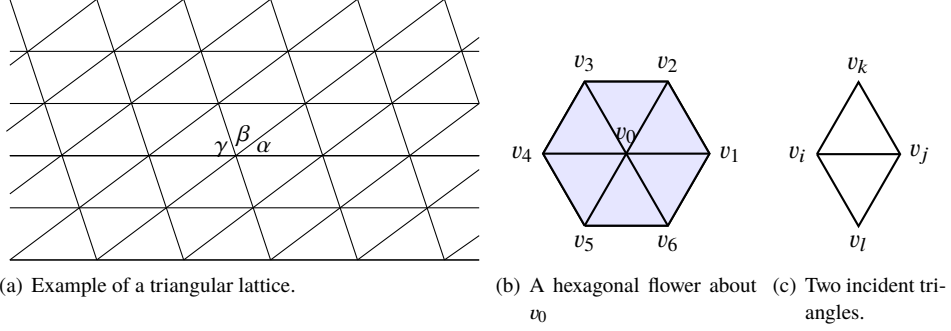


**Figure 2.** Lattice triangulation  $TL_{\mathbb{C}}$  of the plane with congruent triangles, a flower of  $TL_{\mathbb{C}}$  about  $v_0$ , and two incident triangles.

Similarly as for smooth conformal maps, we could demand that  $F$  preserves all cross-ratios, so  $q \equiv Q$ . But then  $\widehat{T}$  is only the image of  $T$  by a Möbius transformation. Therefore, it seems reasonable that only “half” of the cross-ratios remains unchanged, in particular:

**Definition 2.1.** The discrete immersion  $F : T \rightarrow \mathbb{C}$  with image triangulation  $\widehat{T}$  is called *discrete  $\vartheta$ -conformal* for a constant  $\vartheta \in [0, \pi/2]$  if for all interior edges  $[v_i, v_j]$  with adjacent triangles  $\Delta[v_i, v_l, v_j]$  and  $\Delta[v_i, v_j, v_k]$  there holds

$$\operatorname{Re}[e^{-i\vartheta} \log(Q([v_i, v_j]))] = \operatorname{Re}[e^{-i\vartheta} \log(q([v_i, v_j]))], \quad (3)$$

where we assume the values of the logarithm to be in  $\mathbb{R} + i(0, 2\pi)$ .

Note that this definition contains two known notions of discrete conformality based on circle patterns and discrete conformal equivalence.

- For  $\vartheta = 0$  the absolute values of the cross-ratios (length cross-ratios) for adjacent triangles agree, that is  $|Q([v_i, v_j])| = |q([v_i, v_j])|$  holds for all interior edges  $[v_i, v_j]$ . Therefore, the triangulations  $T$  and  $\widehat{T}$  are *discretely conformally equivalent*, see for example [7, Prop. 2.3.2].
- For  $\vartheta = \pi/2$  the arguments of the cross-ratios for adjacent triangles agree, that is  $\arg Q([v_i, v_j]) = \arg q([v_i, v_j])$ . These equal the intersection angles of the corresponding circumcircles. Adding these circumcircles for all triangles in  $T$  and in  $\widehat{T}$ , we obtain a discrete conformal map between two *circle patterns*.

Further properties of discrete  $\vartheta$ -conformal maps will be studied in Sections 4 and 5.

Our considerations in this article are motivated by the study of a class of examples, where the cross-ratios defined in (2) are locally constant. To this end, we restrict ourselves to the case where the triangulation  $T$  is a (part of a) *triangular lattice*  $TL_{\mathbb{C}}$ , that is, a lattice triangulation of the whole complex plane  $\mathbb{C}$  with congruent triangles, see Figure 2(a). We denote the triangulation  $TL = T$  in this case in order to emphasize the lattice structure. For some considerations we need the actual geometric data of the lattice  $TL_{\mathbb{C}}$ , i.e. the angles  $\alpha, \beta, \gamma \in (0, \pi)$  such that  $\alpha + \beta + \gamma = \pi$ , which is specified according to the notation in Figure 2(a). Obviously, the cross-ratios  $Q$  are constant on parallel edges (as  $TL$  is part of a lattice).

We start with a useful property of the cross-ratio function. To this end, we introduce some notation. A vertex  $v_0 \in V$  is called *interior vertex* if it is an interior point of the union of its adjacent closed triangular faces, see Figure 2(b). We call an interior vertex  $v_0$

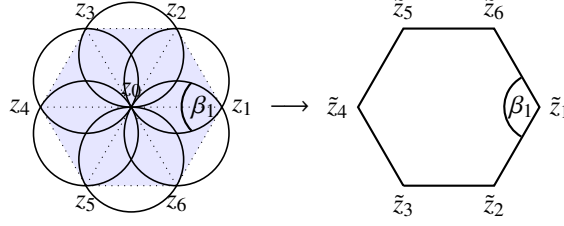


**Figure 3.** Mapping the circumcircles of a flower by a Möbius transformation with  $z_0 \mapsto \infty$

of  $T$  together with its incident triangles (including their vertices and edges) a *flower*. The vertex  $v_0$  is called the *center of the flower* and its neighbors will frequently be enumerated corresponding to the cyclic order of the corresponding vertices of  $T$ .

**Lemma 2.2.** *Let  $TL$  be a part of a triangular lattice. If a function  $q : EL_{int} \rightarrow \mathbb{C} \setminus \mathbb{R}_{\geq 0}$  originates from a discrete immersion of  $TL$  then for every interior vertex  $v_0 \in VL$  with cyclic neighbors  $v_1, \dots, v_6 \in V$  and  $q_k = q([v_0, v_k])$  there holds*

$$\sum_{k=1}^6 \arg(q_k) = 4\pi \quad \Rightarrow \quad q_1 q_2 q_3 q_4 q_5 q_6 = 1, \quad (4)$$

$$1 - q_1 + q_1 q_2 - q_1 q_2 q_3 + q_1 q_2 q_3 q_4 - q_1 q_2 q_3 q_4 q_5 = 0. \quad (5)$$

*Proof.* Given an embedded flower of  $\widehat{TL}$  about  $z_0$ , we add circumcircles to the triangles and then apply a Möbius transformation to this configuration which maps  $z_0$  to  $\infty$  as indicated in Figure 3. As the Möbius transformation does not change the values of the corresponding cross-ratios  $q_k$ , we easily identify equations (4) and (5) as the closing conditions for the image polygon.  $\square$

**Remark 2.3.** Lemma 2.2 is formulated for flowers consisting of six triangles because we are particularly interested in this combinatorics for conformally symmetric triangular lattices. But equations (4) and (5) and their proof can easily be generalized for flowers in arbitrary immersed triangulations  $T$ .

**Remark 2.4.** Given a cross-ratio function  $q$  on the edges of a flower of  $\widehat{TL}$  incident to  $v_0$ , note that equations (4) and (5) are not sufficient to define a discrete embedding of this flower because the interiors of different triangles may intersect. Nevertheless, from the values of  $q$  we can always build a corresponding hexagon as in Figure 3 (right). But this hexagon is possibly not embedded. Applying a Möbius transformation which maps  $\infty$  to a finite point and maps none of the vertices of the hexagon to  $\infty$ , we obtain a configuration of six triangles. These are the images of a piecewise linear map of a flower of  $TL_{\mathbb{C}}$ . By construction, this configuration is unique up to Möbius transformations. In case that the resulting configuration is an embedded flower, we obtain a discrete immersion of this flower. Given further values of the cross-ratio  $q$  on the boundary edges of the flower, these determine new vertices and triangles. If all these triangles are locally embedded about every flower, we can continue this procedure and finally obtain a discrete immersion from the values of the cross-ratio  $q$  on the edges.

## 3. CONFORMALLY SYMMETRIC TRIANGULAR LATTICES

In this section we study conformally symmetric discrete immersions and exploit ideas used in [4] for conformally symmetric circle packings. We choose the cross-ratios of incident triangles as suitable Möbius invariant parameters. Note that throughout this section we will work with (parts of) triangular lattices  $TL$  instead of a general triangulation  $T$ .

The following lemma gives examples of cross-ratio functions as considered in Lemma 2.2 which always lead to discrete immersions.

**Lemma 3.1.** *Let  $q_1, q_2, q_3 \in \mathbb{H} = \{z \in \mathbb{C} : \text{Im}(z) > 0\}$  be three numbers such that  $\arg(q_k) \in (0, \pi)$  and  $\arg(q_1) + \arg(q_2) + \arg(q_3) = 2\pi$ . Define a function  $q : E \rightarrow \{q_1, q_2, q_3\}$  on the edges of a triangular lattice such that  $q$  assumes the same value on parallel edges of  $TL$ . Then there exists a discrete immersion  $\widehat{TL}$ , which will be called generalized Doyle spiral, such that  $q$  is the corresponding cross-ratio function.*

*Proof.* By construction,  $q$  satisfies the necessary conditions (4) and (5) for every flower. Furthermore, the hexagon built corresponding to the values of  $q$  on a flower is symmetric and also embedded as  $q_1, q_2, q_3 \in \mathbb{H}$ . Therefore, there exists a Möbius transformation which maps this hexagon to an embedded flower. In particular, we can take an inversion which maps  $\infty$  to the intersection point of the diagonals of the symmetric hexagon. Then the resulting flower is still symmetric in the following sense: for pair of incident triangles there exists a similarity transformation which maps this pair onto the opposite pair of incident triangles (for example  $\Delta[z_0, z_1, z_2] \cup \Delta[z_0, z_2, z_3]$  onto  $\Delta[z_0, z_4, z_5] \cup \Delta[z_0, z_5, z_6]$  in the notation of Figure 3). Therefore, if we start with such a flower we can continue and use the values of  $q$  to determine further images of vertices as indicated in Remark 2.4. By symmetry, all flowers will be similar and embedded.  $\square$

Doyle spirals carry a lot of symmetry which can be expressed by the fact, that the cross-ratios are constant for all parallel edges of  $TL$ . This is in fact a special case of a *conformally symmetric triangular lattice  $\widehat{TL}$*  which only contains conformally symmetric flowers defined as follows.

**Definition 3.2.** A flower of  $\widehat{TL}$  with center  $y_0 \in \widehat{VL}$  and incident vertices  $z_1, \dots, z_6 \in \widehat{VL}$  in cyclic order is called *conformally symmetric* if there is an involutive Möbius transformation  $M$  with fixed point  $y_0$  and such that

$$M(z_k) = z_{k+3} \text{ for } k \pmod{6}. \quad (6)$$

The Möbius invariant notion of conformal symmetry can locally be characterized as follows.

**Theorem 3.3.** *For any flower in  $\widehat{TL}$  about  $z_0 \in \widehat{V}$  with neighbors  $z_1, \dots, z_6 \in \widehat{V}$  in cyclic order the following statements are equivalent.*

- (i) *The flower is conformally symmetric.*
- (ii) *Opposite cross-ratios agree, that is  $q([v_0, v_k]) = q([v_0, v_{k+3}])$  for  $k = 1, 2, 3$ .*
- (iii) *The circles/lines  $C_k = C_k(z_k, z_0, z_{k+3})$ ,  $k = 1, 2, 3$ , through  $z_k, z_0, z_{k+3}$  have a second common intersection point  $X \in \mathbb{C} \cup \{\infty\}$ , apart from  $z_0$ , which satisfies  $\text{cr}(z_k, z_0, z_{k+3}, X) = -1$ .*

The proof follows by applying suitable Möbius transformations as in the definition of conformal symmetry and is left to the reader.

Note that the statements of this theorem also hold if we replace  $z_0$  by  $X$  for the flower in consideration. But the corresponding flower about  $X$  is not embedded and thus not part of the image of a discrete immersion  $\widehat{TL}$ .

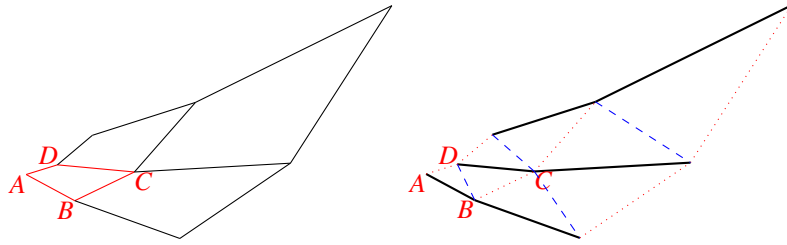


**Figure 4.** Geometric construction of a generalized Doyle spiral and splitting into triangles.

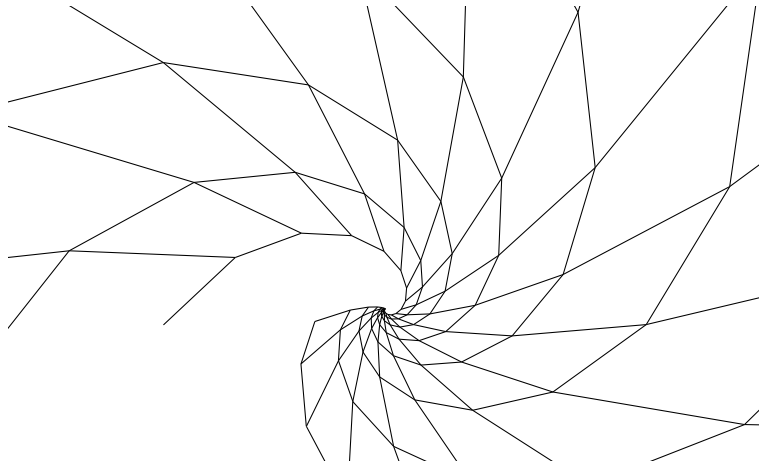


**Figure 5.** Example of a part of a generalized Doyle spiral from a quad.

**3.1. Generalized Doyle spirals.** The study of Doyle spirals began with an observation of Doyle for the construction of circle packing, see [2] for more details. We briefly recall the geometric construction of generalized Doyle spirals which is based on successive gluing of rescaled copies of a given convex quadrilateral.

For a given non-degenerate convex quadrilateral  $Q$  in  $\mathbb{C}$  with vertices  $A, B, C, D$  as in Figure 4 (left), let  $L_1, L_2$  be the orientation preserving similarity transformations such that  $L_1(A) = B, L_1(D) = C, L_2(A) = D, L_2(B) = C$ . Then  $L_2(L_1(Q)) = L_1(L_2(Q))$  by angle count, so  $L_2L_1 = L_1L_2$ . Therefore  $L_1, L_2$  are both translations or both scale-rotations with the same center of rotation. Thus, successive applications of  $L_1, L_2$  generate either a lattice or a generalized Doyle spiral spiraling about the common center, see Figure 5 for an example.

If we split the quadrilateral  $Q$  and all its images consistently into two triangles as in Figure 4 (right), we obtain a triangulation  $\widehat{TL}$  which is the image of a discrete immersion of the whole triangular lattice  $TL_{\mathbb{C}}$ . It is easy to see that the cross-ratios  $q$  defined in (2) are constant on each of the three types of edges and these three values multiply to 1.

**Remark 3.4.** A triangulation  $\widehat{T}$  is a (part of a) generalized Doyle spiral if and only if  $\widehat{T}$  is invariant under the Möbius transformation  $\mathcal{M}$  given in Definition 3.2. This is also equivalent to the fact that all circles  $C_k$  considered in part (iii) of Theorem 3.3 intersect in the same point (the center of the spiral) for all flowers of  $\widehat{T}$ .

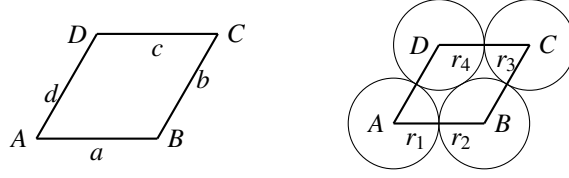


**Figure 6.** Construction of Doyle spirals for circle packings from four mutually tangent circles.

**Remark 3.5** (Connection to Doyle spirals for circle packings). Start with a quadrilateral  $Q$  constructed from the midpoints of four mutually tangent circles (this is possible if and only if  $a + c = b + d$  holds for the edge lengths), see Figure 6. Furthermore, assume that  $L_1$  and  $L_2$  map circles onto circles (which is equivalent to the condition  $r_1 r_3 = r_2 r_4$  for the radii). Then successive applications of  $L_1$  and  $L_2$  to the first four circles will result in a hexagonal circle packing called *Doyle spiral*, see [2].

**Remark 3.6** (Generalized Doyle spirals for conformally equivalent triangulations). For two conformally equivalent triangulations  $TL$  and  $\widehat{TL} = F(TL)$  there exists a function  $u : VL \rightarrow \mathbb{R}$ , called *logarithmic scale factors*, such that the edge lengths are related by  $\widehat{l}([v, w]) = l([vw])e^{(u(v)+u(w))/2}$  for all  $[v, w] \in EL$ , see for example [7]. The logarithmic scale factors for corresponding generalized Doyle spirals on  $TL_C$  with  $VL_C = \{n \sin \alpha_2 + m \sin \alpha_3 e^{i\alpha_1} : n, m \in \mathbb{Z}\}$  are linear,

$$u(n \sin \alpha_2 + m \sin \alpha_3 e^{i\alpha_1}) = An + Bm \quad \text{for suitable } A, B \in \mathbb{R},$$

which indicates that this discrete conformal map can be considered as an analogue of the exponential map. See also [41, Lemma 2.6] and [12].

**3.2. Parametrization of conformally symmetric triangular lattices.** Consider any function  $q : EL_{int} \rightarrow \mathbb{C}$  which satisfies condition (ii) of Theorem 3.3, namely opposite cross-ratios agree,

$$q([v_0, v_k]) = q([v_0, v_{k+3}]), \quad k = 1, 2, 3, \quad (7)$$

for any flower in  $T$ , where  $v_0$  denotes the center with neighbors  $v_1, \dots, v_6$  in cyclic order. Then  $q$  automatically satisfies (5). Combining (7) with (4), we deduce that

$$q([v_0, v_k])q([v_0, v_{k+1}])q([v_0, v_{k+2}]) = 1 \quad (8)$$

for any three consecutive edges in the flower about  $v_0$ . Thus we can describe the general solution of equation (5) together with (7) and (8) as three parameter family on the honeycomb lattice which is dual to the triangular lattice  $TL$ . To this end, consider the function  $q$  (by abuse of notation) to be defined on the corresponding *dual* edges  $e^* \in EL^*$  as in Figure 7.

**Theorem 3.7.** Let  $\widehat{TL}$  be a conformally symmetric triangulation. Define the cross-ratio function  $q : EL_{int} \rightarrow \mathbb{C}$  on the edges and consider it as a function on the dual edges  $q : EL_{int}^* \rightarrow \mathbb{C}$ . Consider an interior dual vertex and denote the corresponding cross-ratios on the incident edges by  $a, b, c \in \mathbb{C} \setminus \mathbb{R}_{\geq 0}$ . Then the dual graph  $\widehat{TL}^*$  is part of a honeycomb lattice and the cross-ratios are given by

$$a_n = a(abc)^{n-1}, \quad b_l = b(abc)^{l-1}, \quad c_m = c(abc)^{m-1} \quad (9)$$

with the notation of Figure 7 (right).



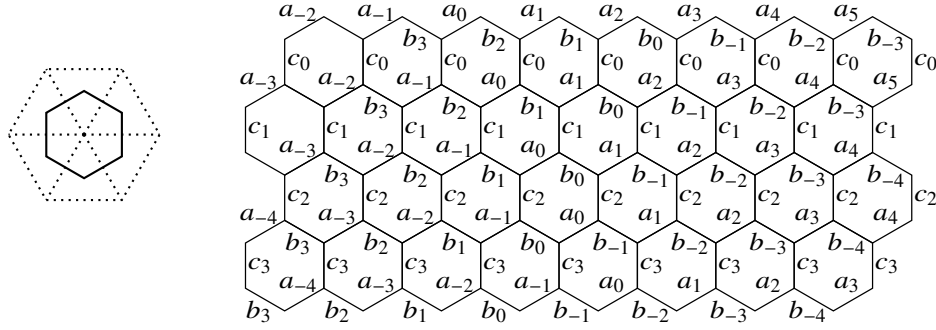


**Figure 7.** *Left:* The edges of a flower (dotted) and the hexagon of their dual edges (black). *Right:* Parametrization of conformally symmetric triangular lattices.

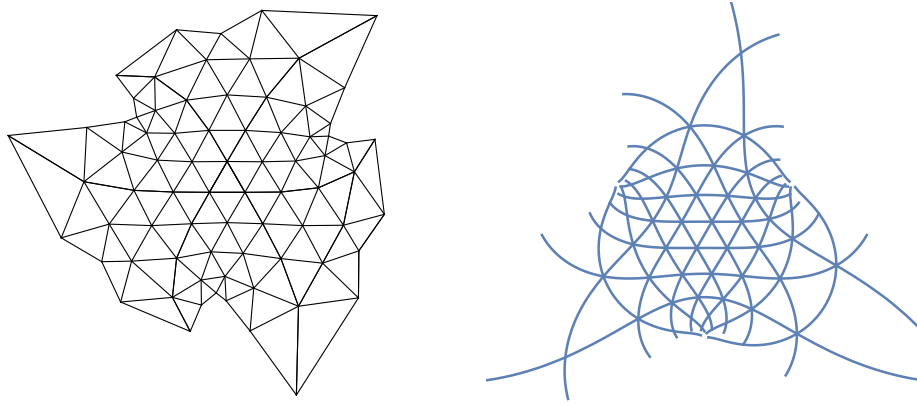


**Figure 8.** *Left:* Example of a general conformally symmetric triangulation with  $a = b = c = e^{i\phi}$  and  $\phi = (2/3 + 1/200)\pi$ . The triangulation already starts to develop singularities. *Right:* Plot of the function  $e^{i\pi/6 \frac{\text{Bi}(w) - \sqrt{3} \cdot \text{Ai}(w)}{\text{Bi}(w) + \sqrt{3} \cdot \text{Ai}(w)}}$

Using this parametrization, we can (locally) construct examples of conformally symmetric discrete immersions.

**Lemma 3.8.** *Let  $a, b, c \in \mathbb{C} \setminus \mathbb{R}_{\geq 0}$ . Assume that there exist three conformally symmetric embedded flowers with the following values of the cross-ratio functions  $q$ :  $a, b, 1/ab$ , and  $a, c, 1/ac$ , and  $c, b, 1/bc$  in counterclockwise orientation respectively. Define a function  $\tilde{q}$  on the whole triangular lattice as in Figure 7 (right) by (9).*

*If  $|abc| = 1$  and  $\arg(a) + \arg(b) + \arg(c) = 2\pi$ , then there exists a generalized Doyle spiral whose cross-ratio function  $q$  agrees with  $\tilde{q}$ .*

*If  $|abc| \neq 1$  or  $\arg(abc) \neq 2\pi$ , then there exists a conformally symmetric discrete immersion whose cross-ratio function  $q$  agrees with  $\tilde{q}$  on this part. But this conformally symmetric discrete immersion cannot be extended to the whole triangular lattice.*

Figure 8 (left) shows an example of a conformally symmetric discrete immersion which is not a Doyle spiral.

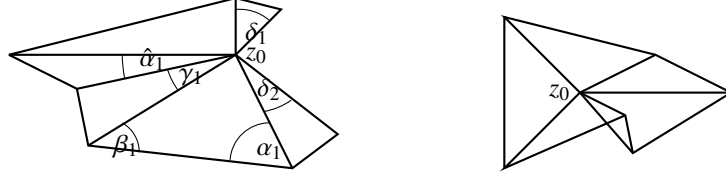


**Figure 9.** Examples of images of a flower about  $z_0$  which does not close up (left) or which contains a non embedded triangle (right)

*Proof.* If  $|abc| = 1$  and  $\arg(a) + \arg(b) + \arg(c) = 2\pi$ , we can start by assumption with an embedded conformally symmetric flower with cross-ratios  $a, b, c$ . As in the proof of Lemma 3.1 we can continue to add triangles according to the given cross-ratios (which are constant on parallel edges) and obtain a generalized Doyle spiral defined on the whole lattice.

If  $|abc| \neq 1$  or  $\arg(abc) \neq 2\pi$  (or both), we still can start by assumption with an embedded conformally symmetric flower and we can continue this discrete immersion (first defined only on one flower) by using the values of  $\tilde{q}$  for the cross-ratios. But we will show that this construction will always lead to non-closing flowers or to non-embedded flowers as in Figure 9. Therefore, we cannot extend the conformally symmetric discrete immersion in this case.

First note that if  $\arg(abc) \neq 2\pi K$  for some  $K \in \mathbb{Z}$ , then we can choose  $n, m \in \mathbb{Z}$  such that with the notation of Figure 7 and (9) we have  $\arg a_n, \arg c_m \in (\pi, 2\pi)$ . But an embedded flower with these cross-ratios  $a_n$  and  $c_m$  (and  $b_{2-n-m}$ ) cannot exist.

If  $abc = |abc| \neq 1$ , we may assume that  $\arg(a) + \arg(b) + \arg(c) = 2\pi$  holds for  $\arg(a), \arg(b), \arg(c) \in (0, 2\pi)$  because else we do not obtain an embedded flower (which we have by assumption). As  $|abc| \neq 1$  there exist  $n, m, l$  such that  $|a_n| > C, |b_l| > C$  and  $|c_m| > C$  for any constant  $C > 0$ . Therefore, if one of the arguments of  $a, b, c$  is  $> \pi$ , we can choose two of the indices and consider a flower with two very big length cross-ratios such that the hexagon corresponding to these cross-ratios as in Figure 3 (right) is not embedded. In this case, the corresponding flower will also be non-embedded, see Figure 9. So the only remaining case is  $\arg(a), \arg(b), \arg(c) \in (0, \pi]$ . Assume without loss of generality that  $\arg b \leq \arg c < \pi$ . Let  $n$  be such that  $|a_n| > 1/\sin^2((\pi - \arg b)/2)$  and assume that  $|a_n|$  is very large. Consider a pair of embedded triangles with cross-ratio  $a_n$  on the edge, then one of the adjacent angles is smaller than  $\arcsin(1/\sqrt{|a_n|})$ . Call this angle  $\gamma_1$  and consider the notation of Figure 9 (left). As the configuration is assumed to be embedded we deduce  $\hat{\alpha}_1 \leq \arcsin(1/|c_m|)$ . Note that we can also choose  $|c_m|$  as large as we like if we suppose that we have a conformally symmetric discrete immersion on the whole triangular lattice. But as  $\pi - \alpha_1 - \beta_1 < \arg b$ , we can choose  $n, m$  such that  $\gamma_1, \hat{\alpha}_1$  and similarly  $\delta_1, \delta_2$  are so small that  $2\arg(b) + \gamma_1 + \hat{\alpha}_1 + \delta_1 + \delta_2 < 2\pi$ . Therefore, the flower cannot close up about  $z_0$ .  $\square$

**Corollary 3.9.** *Generalized Doyle spirals are the only conformally symmetric triangular meshes of the whole lattice.*

**3.3. Smooth analogues for conformally symmetric triangular lattices.** In the following, we are interested in identifying the smooth conformal maps which may be considered as analogues of conformally symmetric immersions. Many examples of conformally symmetric discrete immersions are discrete  $\vartheta$ -conformal maps for some  $\vartheta \in [0, \pi/2]$  which will be

detailed in Subsection 4.1. The main idea for relating our conformally symmetric discrete immersions to smooth analogues is to consider the function  $\log(q([v_0, v_k])/Q([v_0, v_k]))$  as a discrete version of the Schwarzian derivative, similarly as in [4] for conformally symmetric circle packings. A similar approach has been taken in [13] where a more detailed connection of discrete and smooth Schwarzian derivatives is established via convergence statements, but only for the cases of conformal equivalence ( $\vartheta = 0$ ) and circle patterns ( $\vartheta = \pi/2$ ).

Recall that  $Q$  is constant on parallel edges due to the symmetry of the lattice. Thus generalized Doyle spirals with constant values of  $q$  on parallel edges corresponds to a constant Schwarzian derivative and can therefore be considered as discrete exponentials. In the remaining case of conformally symmetric discrete immersions we know from (9) that  $q$  is constant along lattice directions which corresponds to a linear Schwarzian derivative. In the smooth theory, conformal maps with linear non-constant Schwarzian derivative are quotients of Airy functions (see Figure 8 (right) for an example). Airy functions are fundamental solutions of  $\psi'' = x\psi$ , see for example [37], in particular

$$\text{Ai}(x) = \frac{1}{\pi} \int_0^\infty \cos(xt + \frac{t^3}{3}) dt, \quad \text{Bi}(x) = \frac{1}{\pi} \int_0^\infty e^{xt - \frac{t^3}{3}} + \sin(xt + \frac{t^3}{3}) dt.$$

Therefore, conformally symmetric discrete immersions can be considered as discrete analogues of quotients of Airy functions.

#### 4. EXAMPLES OF DISCRETE $\vartheta$ -CONFORMAL MAPS AND CONNECTION TO TRIGONOMETRY

Our study of conformally symmetric triangulations motivated the introduction of discrete  $\vartheta$ -conformal maps. In this section, we show that many conformally symmetric triangular lattices constitute examples of  $\vartheta$ -conformal maps. Furthermore, we show how discrete  $\vartheta$ -conformal maps may be related to discrete holomorphic differentials. Finally, we present some geometric ideas related to the notion of  $\vartheta$ -conformal maps.

**4.1. Conformally symmetric triangular lattices as examples of discrete  $\vartheta$ -conformal maps.** The class of conformally symmetric triangular lattices provides examples for all discrete  $\vartheta$ -conformal maps in the sense of Definition 2.1.

We start with generalized Doyle spirals. We will now prove that generalized Doyle spirals constitute examples of discrete  $\vartheta$ -conformal maps for suitable triangular lattices and suitable choices for  $\vartheta$ .

**Lemma 4.1.** *For every generalized Doyle spiral where all quadrilaterals have been split consistently into triangles, there exists an interval  $I \subset [0, \frac{\pi}{2}]$ , where  $I = (\vartheta_0, \frac{\pi}{2}]$  for some  $\vartheta_0 \in [0, \frac{\pi}{2}]$  or  $I = [0, \frac{\pi}{2}]$ , such that for every  $\vartheta \in I$  there is a triangular lattice  $TL_{\mathbb{C}} = TL_{\mathbb{C}}(\vartheta)$  and a discrete  $\vartheta$ -conformal map  $F : TL_{\mathbb{C}} \rightarrow \mathbb{C}$  such that the image of  $TL_{\mathbb{C}}$  under  $F$  is the given generalized Doyle spiral.*

*Proof.* Given a generalized Doyle spiral, split all of its convex quadrilaterals consistently into triangles as in Figure 4 (right). This defines six angles  $\alpha_1, \dots, \alpha_6 \in (0, \pi)$  as in Figure 10 which determine the quads of the Doyle spiral up to Euclidean motions and scaling. Due to the convexity of the quad, these six angles satisfy  $\alpha_3 + \alpha_6 < \pi$ ,  $\alpha_2 + \alpha_4 < \pi$ ,  $\alpha_1 + \alpha_2 + \alpha_3 = \pi$ , and  $\alpha_4 + \alpha_5 + \alpha_6 = \pi$  and they determine the cross-ratios  $q_1, q_2, q_3$  of the

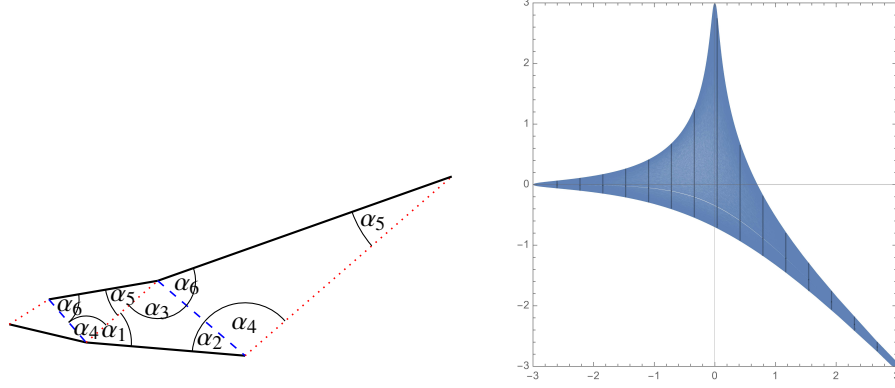


**Figure 10.** *Left:* Definition of angles in the splitted convex quads of a generalized Doyle spiral; *right:* Image domain of  $G(\alpha, \beta)$

Doyle spiral via

$$\begin{aligned}\log q_1 &= \log \left( \frac{\sin \alpha_6}{\sin \alpha_4} \cdot \frac{\sin \alpha_2}{\sin \alpha_3} \right) + i(\alpha_1 + \alpha_5), \\ \log q_2 &= \log \left( \frac{\sin \alpha_3}{\sin \alpha_1} \cdot \frac{\sin \alpha_4}{\sin \alpha_5} \right) + i(\alpha_2 + \alpha_6), \\ \log q_3 &= \log \left( \frac{\sin \alpha_5}{\sin \alpha_6} \cdot \frac{\sin \alpha_1}{\sin \alpha_2} \right) + i(\alpha_3 + \alpha_4).\end{aligned}$$

The labeling of the cross-ratios is defined according to these formulas.

Let  $TL_C$  be a triangular lattice with angles  $\alpha, \beta, \gamma \in (0, \pi)$  as in Figure 2(a), where  $\alpha + \beta + \gamma = \pi$ . Then its three cross-ratios may be expressed in terms of the angles as

$$\log Q_1 = 2 \log \frac{\sin \beta}{\sin \alpha} + 2i\gamma, \quad \log Q_2 = 2 \log \frac{\sin \alpha}{\sin \gamma} + 2i\beta, \quad \log Q_3 = 2 \log \frac{\sin \gamma}{\sin \beta} + 2i\alpha.$$

Thus, for  $\vartheta = \pi/2$  we can choose  $\gamma = (\alpha_1 + \alpha_5)/2$ ,  $\beta = (\alpha_2 + \alpha_6)/2$ , and  $\alpha = (\alpha_3 + \alpha_4)/2$  and obtain  $\operatorname{Re}(e^{-i\frac{\pi}{2}} q_k) = \operatorname{Re}(e^{-i\frac{\pi}{2}} Q_k)$  for  $k = 1, 2, 3$ . Also, at least for  $\vartheta$  in a small neighborhood of  $\pi/2$ , the equations  $\operatorname{Re}(e^{-i\vartheta} q_k) = \operatorname{Re}(e^{-i\vartheta} Q_k)$  are still solvable in terms of  $\alpha, \beta, \gamma$  for given  $\alpha_1, \dots, \alpha_6$  as above. But the image of  $\{(\alpha, \beta) \in (0, \pi)^2 : \alpha + \beta < \pi\}$  under

$$G(\alpha, \beta) = \begin{pmatrix} \log \frac{\sin \beta}{\sin \alpha} \\ \log \frac{\sin \alpha}{\sin(\alpha+\beta)} \end{pmatrix}$$

is not convex, see Figure 10 (right) (compare also to [7, Fig. 9]). Thus, there exist configurations with angles  $\alpha_1, \dots, \alpha_6 \in (0, \pi)$  as in Figure 10 such that the system  $G(\alpha_4, \alpha_6) + G(\alpha_3, \alpha_2) = 2G(\alpha, \beta)$  has no solution  $\alpha, \beta \in (0, \pi)$  with  $\alpha + \beta < \pi$ . This is equivalent to the fact that for such a configuration the system of equations  $\operatorname{Re}(\log q_k) = \operatorname{Re}(\log Q_k)$ ,  $k = 1, 2, 3$  have no solution for  $Q_k$ , which means that there is no corresponding triangular lattice  $TL_C$  such that the discrete immersion from  $TL_C$  to the generalized Doyle spiral is discrete  $\vartheta$ -conformal for this  $\vartheta$ . Thus, depending on the given generalized Doyle spiral, the interval for suitable  $\vartheta$ 's may in some cases be strictly smaller than  $[0, \pi/2]$ .  $\square$

**Remark 4.2.** In the theory of conformally equivalent triangular lattices, a change of the combinatorics by means of edge flipping is required in order to guarantee the existence of solutions, see [24, 38]. Lemma 4.1 suggests that such combinatorial changes may also be necessary for discrete  $\vartheta$ -conformal maps. This demonstrates that discrete  $\vartheta$ -conformal maps, which interpolate between circle patterns and conformally equivalent triangulations, inherit properties from both theories. A change of the combinatorics could also prevent triangles and flowers from being degenerate as considered in the proof of Lemma 3.8.

The proof of Lemma 4.1 actually shows that if the angles of the split quads are all in a suitable neighborhood of  $\pi/3$  then the corresponding generalized Doyle spirals are discrete  $\vartheta$ -conformal maps for all  $\vartheta \in [0, \pi/2]$ . This observation motivated the introduction and study of discrete  $\vartheta$ -conformal maps.

Furthermore, we can map every flower of a generalized Doyle spiral by a Möbius transformation to a symmetric embedded flower in the sense that  $\mathcal{M}(z_j) = -\mathcal{M}(z_{j+3})$ . Then we can observe that the generalized Doyle spiral is discrete  $\vartheta$ -conformal for every  $\vartheta \in [0, \pi/2]$  if and only if this symmetric flower is convex.

Apart from Doyle spirals, we know from Lemma 3.8 that a conformally symmetric discrete immersion is only defined on a part  $TL$  of the lattice  $TL_{\mathbb{C}}$  and its cross-ratio function  $q$  is given by (9) on the corresponding part of the hexagonal lattice indicated in Figure 7. In particular, the proof of Theorem 3.7 shows that for the part of the lattice where the conformally symmetric discrete immersion is defined, we have  $\log a_n = \log a + (n - 1) \log(abc)$  and analogous formulas for  $\log b_l$  and  $\log c_m$ .

Therefore we deduce that

- if  $|abc| = 1$ , then  $\operatorname{Re}(\log a_n) = \operatorname{Re}(\log a) = |a|$  and analogously for  $\log b_l$  and  $\log c_m$ . If there exists a triangular lattice with length cross-ratios  $|a|, |b|, |c|$  (see the proof of Lemma 4.1 for this issue), then the conformally symmetric discrete immersion is discrete  $\vartheta$ -conformal for  $\vartheta = 0$ .
- if  $abc \in \mathbb{R}_+ = (0, \infty)$  or equivalently  $\arg(a) + \arg(b) + \arg(c) = 2\pi$ , the circle pattern obtained from adding the circumcircles to all triangles has the same intersection angles as the circle pattern built from the circumcircles of the triangles in the lattice  $TL_{\mathbb{C}}$  with angles  $\alpha = \arg(a)/2$ ,  $\beta = \arg(b)/2$  and  $\gamma = \arg(c)/2$ . In this case, the conformally symmetric discrete immersion is discrete  $\vartheta$ -conformal for  $\vartheta = \pi/2$ .
- if  $\operatorname{Re}(e^{-i\vartheta} \log(abc)) = 0$  or equivalently  $\cos \vartheta \log |abc| + \sin \vartheta \arg(abc) = 0$  for some  $\vartheta \in (0, \pi/2)$ , this may be an example of a general discrete  $\vartheta$ -conformal map. In fact, this is the case if there exists a triangular lattice  $TL_{\mathbb{C}}$  whose cross-ratio function  $Q$  satisfies  $\operatorname{Re}(e^{-i\vartheta} \log Q_1) = \operatorname{Re}(e^{-i\vartheta} \log a)$ ,  $\operatorname{Re}(e^{-i\vartheta} \log Q_2) = \operatorname{Re}(e^{-i\vartheta} \log b)$ , and  $\operatorname{Re}(e^{-i\vartheta} \log Q_3) = \operatorname{Re}(e^{-i\vartheta} \log c)$ , where  $Q_1, Q_2, Q_3$  denote the three (in general different) values of the cross-ratio function  $Q$  on the lattice  $TL_{\mathbb{C}}$ .

Combining this reasoning with Corollary 3.9, we obtain the following immediate consequence.

**Corollary 4.3.** *Generalized Doyle spirals are the only conformally symmetric triangular meshes from discrete  $\vartheta$ -conformal maps of the whole lattice.*

**4.2. Connection to discrete holomorphic quadratic differentials.** For any smooth one parameter family  $g(t) : T \rightarrow \mathbb{C}$ ,  $t \in (-\varepsilon, \varepsilon)$ , of discrete immersions of a simply connected triangulation the considerations and results for infinitesimal deformations of [29, Section 5] apply. In particular, the corresponding cross-ratio functions  $q(t)$  on the interior edges is a perturbation of  $q(0) \equiv Q$  for some general immersed triangulation  $T$ . The logarithmic

derivatives

$$q_{ij} := \frac{1}{q(0)([v_i, v_j])} \frac{d}{dt} \Big|_{t=0} q(t)([v_i, v_j]) \quad (10)$$

on the interior edges  $[v_i, v_j] \in E$  satisfy

$$\sum_{v_j: v_j \text{ adjacent to } v_i} q_{ij} = 0 \quad \text{and} \quad \sum_{v_j: v_j \text{ adjacent to } v_i} \frac{q_{ij}}{v_i - v_j} = 0. \quad (11)$$

This is a consequence of the generalized versions of (4) and (5) explained in Remark 2.3 by taking derivatives, see also [29, Cor. 5.3]. Furthermore, for a family  $g(t)$  of discrete  $\vartheta$ -conformal maps we deduce that  $q_{ij} \in ie^{i\vartheta}\mathbb{R}$ . This is analogous to the two cases for conformal equivalence ( $q_{ij} \in i\mathbb{R}$ ) and circle patterns ( $q_{ij} \in \mathbb{R}$ ) considered in [29]. Therefore we may also call  $q_{ij}$  a *discrete holomorphic quadratic differential*. In view of [28], we can interpret the cases for  $\vartheta \neq 0, \pi/2$  as corresponding to the associated family of minimal surfaces.

For the special example of generalized Doyle spirals, a one parameter family of discrete  $\vartheta$ -conformal maps which are generalized Doyle spirals may be easily constructed explicitly. Start with a triangular lattice  $TL$  with cross-ratio function  $Q : EL \rightarrow \{A, B, C\} \subset \mathbb{C} \setminus \mathbb{R}_{\leq 0}$ . In particular,  $ABC = 1$ . For  $\vartheta \in [0, \pi/2]$ , set  $R(A, \vartheta) = \operatorname{Re}[e^{-i\vartheta} \log(A)]$  and  $I(A, \vartheta) = \operatorname{Im}[e^{-i\vartheta} \log(A)]$  and define  $R(B, \vartheta)$ ,  $R(C, \vartheta)$  and  $I(B, \vartheta)$ ,  $I(C, \vartheta)$  analogously. Let  $a, b, c \in \mathbb{C} \setminus \mathbb{R}_{\leq 0}$  be the cross-ratio function of another triangular lattice. Then there exists a one parameter family of generalized Doyle spirals  $\widehat{T}(t)$  with cross-ratio function  $q(t) : EL \rightarrow \{q_A(t), q_B(t), q_C(t)\}$ , where

$$q_A(t) = \exp(R(A, \vartheta)e^{i\vartheta} + ie^{i\vartheta}(t\operatorname{Im}[e^{-i\vartheta} \log(a)] + (1-t)I(A, \vartheta)))$$

and  $q_B(t)$  and  $q_C(t)$  are defined analogously. The logarithmic derivatives  $q_{ij}$  defined by (10) satisfy (11) and additionally  $\sum_{[v_j, v_i] \text{ incident to triangle } \Delta} q_{ij} = 0$  for all triangular faces  $\Delta$  of  $TL_{\mathbb{C}}$ .

This last property means that this discrete holomorphic quadratic differential is *integrable*.

**Corollary 4.4.** *Every integrable discrete holomorphic quadratic differential on a triangular lattice  $TL_{\mathbb{C}}$  arises from a one parameter family of discrete  $\vartheta$ -conformal maps which are generalized Doyle spirals.*

**4.3. Trigonometry with parameter  $\vartheta$ .** It is well known that a triangle is determined up to similarity transformations by its angles or by the ratios of its edge lengths. These two well known examples will correspond to our cases  $\vartheta = 0$  and  $\vartheta = \pi/2$ . For  $\vartheta \in (0, \pi/2)$  we switch to unusual parameters for the construction of triangles.

As for the definition of the cross-ratio in (1), we mainly focus on notions based on differences like  $w_{ij} = v_j - v_i$  etc. These are associated to directed edges of the embedded non-degenerate counterclockwise oriented triangles  $\Delta[v_i, v_j, v_k]$  of the given triangulation  $T$ . Similarly, we consider the directed edges  $z_{ij} = z_j - z_i$  of the non-degenerate image triangles  $F(\Delta[v_i, v_j, v_k]) = \Delta[z_i, z_j, z_k]$  for any discrete immersion  $F$ . These complex numbers satisfy the obvious closing condition  $z_{ij} + z_{jk} + z_{ki} = 0$ . This algebraic equation is naturally studied in  $\mathbb{C}P^2$  and this means that we consider triangles up to global similarity transformations which does not change the cross-ratios  $q$ . When dealing with similarity classes of embedded triangles, one natural approach is to work with the quotients  $\tau_k^{ij} = z_{kj}/z_{ki} \in \mathbb{H} = \{z \in \mathbb{C} : \operatorname{Im}(z) > 0\}$  in the upper half-plane of  $\mathbb{C}$  or their logarithms  $\log \tau_k^{ij}$  as for example in [14, Section 1.5]. They satisfy the relations  $\tau_k^{ij} \tau_i^{jk} \tau_j^{ki} = -1$  and  $\tau_j^{ki} \tau_i^{jk} = \tau_k^{ij} - 1$ . Thus, if we denote  $\tau_k^{ij} = \tau$  we have  $\tau_i^{jk} = 1/(1 - \tau)$  and  $\tau_j^{ki} = 1 - 1/\tau$ .

Furthermore, their logarithms satisfy

$$\log \tau_k^{ij} + \log \tau_i^{jk} + \log \tau_j^{ki} = \pi i. \quad (12)$$

In view of (3), we choose to work with these logarithmic variables. As scale-rotations may be parametrized via  $z \mapsto z \cdot e^A$  for  $A \in \mathbb{C}$ , these variables belong to the Lie algebra of scale-rotations and are usually split into real and imaginary parts which correspond to scaling and rotation respectively. The right hand side of (12) fits to this splitting. For our purposes we choose another orthonormal basis of this Lie algebra, namely  $e^{i\vartheta}$  and  $ie^{i\vartheta}$ . To simplify further considerations, we introduce parameters relative to a given configuration. In particular, instead of  $\log \tau_k^{ij} = \log(z_{kj}/z_{ki})$ , we focus on  $\zeta_k^{ij} = \log\left(\frac{z_{kj}}{z_{ki}} \frac{w_{ki}}{w_{kj}}\right) := \log \frac{z_{kj}}{z_{ki}} - \log \frac{w_{kj}}{w_{ki}}$ . These variables satisfy

$$\zeta_k^{ij} + \zeta_i^{jk} + \zeta_j^{ki} = 0. \quad (13)$$

and we will split them according to the orthonormal basis  $e^{i\vartheta}$  and  $ie^{i\vartheta}$ , that is  $\zeta_k^{ij} = \log\left(\frac{z_{kj}}{z_{ki}} \frac{w_{ki}}{w_{kj}}\right) = e^{i\vartheta}(i\hat{\zeta}_{ij} + \hat{\zeta}_{ij})$  with real  $\hat{\zeta}_{ij}, \hat{\zeta}_{ij} \in \mathbb{R}$ . In the triangular graph  $G_M^\Delta$  whose vertices are the midpoints  $M_{ij} = (v_i + v_j)/2$  of the edges  $[v_i, v_j]$  of the triangle  $\Delta[v_i, v_j, v_k]$ , the variables  $\hat{\zeta}_{ij} = -\hat{\zeta}_{ji}$  and  $\hat{\zeta}_{ij} = -\hat{\zeta}_{ji}$  may be interpreted as a 1-form on the edges  $[M_{kj}, M_{ki}]$ . Condition (13) shows that this 1-form is closed. Therefore, we can integrate and obtain  $\zeta_k^{ij} = e^{i\vartheta}(i(\omega_{kj} - \omega_{ki}) + (v_{kj} - v_{ki}))$ . The real variables  $\omega_{ij}, v_{ij} \in \mathbb{R}$  are associated to the midpoints  $M$  and thus to the original edges of the triangle  $\Delta[v_i, v_j, v_k]$ . They are unique up to a common constant, respectively. Furthermore, if we switch back to our original triangles  $\Delta[v_i, v_j, v_k]$  and  $\Delta[z_i, z_j, z_k]$ , we deduce that by a suitable choice of these constants we can express

$$z_{ij} = w_{ij} \cdot \exp(e^{i\vartheta}(i\omega_{ij} + v_{ij})). \quad (14)$$

Thus,  $\exp(e^{i\vartheta}(i\omega_{ij} + v_{ij}))$  describes the scale-rotation which transforms  $w_{ij}$  into  $z_{ij}$ . For  $\vartheta = \pi/2$ , the variables  $\omega_{ij} = \log|z_{ij}| - \log|w_{ij}|$  and  $v_{ij} = \arg(z_{ij}) - \arg(w_{ij})$  are just the (negative) logarithmic scale factor of the edge  $z_{ij}$  and its relative rotation angle with respect to  $w_{ij}$ . This holds also true for  $\vartheta = 0$  where the roles of logarithmic scale factor and rotation angle are interchanged. In fact for  $\vartheta \in (0, \pi/2)$ , the new variables  $\omega_{ij}, v_{ij}$  are linear combinations of these two known parameters. Note that the values of  $\omega_{ij}$  and/or  $v_{ij}$  are not uniquely defined in  $\mathbb{R}$  by (14). The same result is obtained for  $\omega_{ij} + 2\pi \cos \vartheta \cdot K$  and  $v_{ij} + 2\pi \sin \vartheta \cdot K$  for any  $K \in \mathbb{Z}$ . In order to simplify our calculations, we will always choose the values  $\omega_{ij}, v_{ij}$  such that the angle  $\alpha_k^{\Delta[z_i, z_j, z_k]}$  in the image triangle  $\Delta[z_i, z_j, z_k]$  at the vertex  $z_k$  can be expressed as

$$\alpha_k^{\Delta[z_i, z_j, z_k]} = \alpha_k^{\Delta[v_i, v_j, v_k]} + \cos \vartheta (\omega_{ki} - \omega_{jk}) + \sin \vartheta (v_{ki} - v_{jk}). \quad (15)$$

This defines our variables at the given triangle uniquely up to a global constant, which will not be important for our considerations as we mainly work with differences.

## 5. A VARIATIONAL PRINCIPLE FOR DISCRETE $\vartheta$ -CONFORMAL MAPS

Recall that  $T$  is an immersed triangulation in the plane. For simplicity, we assume that  $T$  is simply connected. Let  $F : T \rightarrow \mathbb{C}$  be a discrete immersion with image  $\widehat{T}$ . In this section we prove the existence of a variational principle for discrete  $\vartheta$ -conformal maps.

Similarly as for circle patterns and conformally equivalent triangulations, discrete  $\vartheta$ -conformal maps are associated to a special description of triangles which has been introduced in Section 4.3. We use this for a reformulation of condition (3) which in turn will be shown to be a partial derivative of a locally defined functional  $\mathcal{F}_\vartheta(\omega)$ . Thus we aim at the following theorem, which is a direct consequence of Theorems 5.3–5.5 below.

**Theorem 5.1.** *For any discrete  $\vartheta$ -conformal map  $F : T \rightarrow \widehat{T}$ , the corresponding variables  $\omega \in \mathbb{R}^{|E|}$  constitute the unique maximizer (up to a global constant) of a locally concave functional  $\mathcal{F}_\vartheta$ .*

*Conversely, every maximizer of  $\mathcal{F}_\vartheta$  on a simply connected triangulation  $T$  corresponds to a  $\vartheta$ -conformal map  $F : T \rightarrow \widehat{T}$ .*

**5.1. A single triangle in new variables.** As in Section 4.3, let  $w_{ij} = v_j - v_i$  denote the directed edges of an embedded non-degenerate triangle  $\Delta[v_i, v_j, v_k]$ . Similarly, we consider the directed edges  $z_{ij} = z_j - z_i$  of the non-degenerate image triangles  $F(\Delta[v_i, v_j, v_k]) = \Delta[z_i, z_j, z_k]$  for any discrete immersion  $F$ . Now, we express the obvious closing condition  $z_{ij} + z_{jk} + z_{ki} = 0$  as

$$w_{ij} \cdot \exp(e^{i\vartheta}(i\omega_{ij} + \nu_{ij})) + w_{jk} \cdot \exp(e^{i\vartheta}(i\omega_{jk} + \nu_{jk})) + w_{ki} \cdot \exp(e^{i\vartheta}(i\omega_{ki} + \nu_{ki})) = 0. \quad (16)$$

In the following, we consider the  $\omega$ 's as our main variables and the  $\nu$ 's as dependent functions. By the implicit function theorem, we can assume that the  $\nu$ 's depend smoothly on the given variables  $\omega$  in a suitable neighborhood of a solution.

As in the cases for given edge lengths or angles, not all choices of  $\omega$ 's correspond to a triangle. This means, that for some choices of  $\omega$ 's there do not exist any real  $\nu$ 's such that (16) holds. We briefly describe the set of suitable choices of  $\omega$ 's for the normalized case  $z_{ij} = w_{ij} = 1$ ,  $z_{jk} = w_{jk} \cdot \exp(e^{i\vartheta}(i\omega_1 + \nu_1)) =: w_{jk} \cdot \sigma_1$  and  $z_{ki} = w_{ki} \cdot \exp(e^{i\vartheta}(i\omega_2 + \nu_2)) =: w_{ki} \cdot \sigma_2$ .

Associate to a non-zero complex number  $w$  the set  $S_w = \{(\log |w|, \arg w + 2\pi k) : k \in \mathbb{Z}\} \subset \mathbb{R}^2$  of all values of the logarithm  $\log w$  (i.e. possible polar coordinates). We apply the map  $w \mapsto S_w$  to the edge of the image triangle and consider in particular  $L : (\sigma_1, \sigma_2) \mapsto S_{\sigma_1} \times S_{\sigma_2}$ . Then the set  $E_\vartheta$  of all suitable choices for  $\omega_1, \omega_2$  is the intersection of the plane in  $\mathbb{C}^2 \cong \mathbb{R}^4$  generated by  $\begin{pmatrix} -\sin \vartheta \\ \cos \vartheta \end{pmatrix} \times \{0\}$  and  $\{0\} \times \begin{pmatrix} -\sin \vartheta \\ \cos \vartheta \end{pmatrix}$  with the image of the set  $\{(\sigma_1, \sigma_2) \in \mathbb{C}^2 : 1 + w_{jk} \cdot \sigma_1 + w_{ki} \cdot \sigma_2 = 0 \text{ and } w_{jk} \cdot \sigma_1, -w_{ki} \cdot \sigma_2 \in \mathbb{H}\}$  under the map  $L$ . As all sets  $S_w$  have a translational period of  $2\pi$  in the second component, the set  $E_\vartheta$  is  $(2\pi \cos \vartheta)$ -periodic if  $\vartheta \neq \pi/2$ . By the inverse function theorem, we easily deduce that the set  $E_\vartheta$  is open.

**Remark 5.2.** Consider as above the normalized directed edges  $z_{ij} = w_{ij} = 1$ ,  $z_{jk} = w_{jk} \cdot \exp(e^{i\vartheta}(i\omega_1 + \nu_1))$ ,  $z_{ki} = w_{ki} \cdot \exp(e^{i\vartheta}(i\omega_2 + \nu_2))$  which (possibly) build a non-degenerate triangle with counterclockwise orientation. In this description, the existence of suitable  $\nu_1, \nu_2$  for given  $\omega_1, \omega_2$  is equivalent to the fact that the two spirals  $s_1(t) = a \cdot \exp(e^{i\vartheta} t)$  and  $s_2(t) = b \cdot \exp(e^{i\vartheta} t)$ , where  $a = w_{jk} \cdot \exp(i e^{i\vartheta} \omega_1)$ ,  $b = w_{ki} \cdot \exp(i e^{i\vartheta} \omega_2)$  and  $t \in \mathbb{R}$ , intersect transversally in the upper half-plane  $\mathbb{H}$ . Depending on  $a$  and  $b$ , there may exist several intersection points for some values of  $\omega_1, \omega_2$ . In these cases, we obtain several (smooth) functions  $\nu_j(\omega)$ .

If we only consider (small) variations of a given configuration, we may assume that  $\omega$ , and thus  $\nu$ , is in a neighborhood of zero and therefore obtain a well-defined function  $\nu(\omega)$ . In the general case, we have to consider several functions  $\nu^{(l)}(\omega)$  on different, overlapping domains.



**5.2. Condition for discrete  $\vartheta$ -conformal maps in new variables.** Our next goal is to reformulate condition (3). To this end, it is sufficient to consider the embedded configuration of two adjacent triangles  $\Delta[v_i, v_j, v_k]$  and  $\Delta[v_i, v_l, v_j]$  and their images  $F(\Delta[v_i, v_j, v_k]) = \Delta[z_i, z_j, z_k]$  and  $F(\Delta[v_i, v_l, v_j]) = \Delta[z_i, z_l, z_j]$  for any discrete immersion  $F$ . The cross-ratios  $q_{ij} = q([v_i, v_j])$  defined by (2) can be expressed as

$$q_{ij} = \frac{w_{il}w_{jk}}{w_{lj}w_{ki}} \cdot \frac{\exp(e^{i\vartheta}(i\omega_{il} + \nu_{il}))}{\exp(e^{i\vartheta}(i\omega_{lj} + \nu_{lj}))} \cdot \frac{\exp(e^{i\vartheta}(i\omega_{jk} + \nu_{jk}))}{\exp(e^{i\vartheta}(i\omega_{ki} + \nu_{ki}))}. \quad (17)$$

As  $Q([v_i, v_j]) = \frac{w_{il}w_{jk}}{w_{lj}w_{ki}}$  we deduce that

$$e^{-i\vartheta} \log q_{ij} = e^{-i\vartheta} \log Q([v_i, v_j]) + i(\omega_{il} - \omega_{lj} + \omega_{jk} - \omega_{ki}) + \nu_{il} - \nu_{lj} + \nu_{jk} - \nu_{ki}.$$

Thus  $F$  is discrete  $\vartheta$ -conformal on this minimal example of two adjacent triangles if and only if

$$\nu_{il} - \nu_{lj} + \nu_{jk} - \nu_{ki} = 0 \quad (18)$$

holds.

Recall that the  $\nu$ 's depend on the variables  $\omega$  in the respective triangles. We will emphasize this by writing  $\nu_{il}^{\Delta[v_i, v_l, v_j]}$  etc. In particular, the two values of  $\nu$  associated to the same edge will in general be different:  $\nu_{ij}^{\Delta[v_i, v_l, v_j]} \neq \nu_{ij}^{\Delta[v_i, v_j, v_k]}$ .

**5.3. Brief review on the known cases for  $\vartheta = 0$  and  $\vartheta = \pi/2$ .** The abstract variables  $\omega_{ij}$  and  $\nu_{ij}$  and condition (18) become geometrically more specific if we consider the case of circle patterns ( $\vartheta = \pi/2$ ) and conformally equivalent triangulations ( $\vartheta = 0$ ). As in the general case studied in Section 4.3, we regard the embedded, counterclockwise oriented triangle  $\Delta[z_i, z_j, z_k]$  as obtained from a given (embedded, counterclockwise oriented) triangle  $\Delta[v_i, v_j, v_k]$  and consider the relative changes of the directed edges, edge lengths and angles.

**5.3.1. Circle patterns.** In the case  $\vartheta = \pi/2$ , the free variables  $\omega_{ij}$  are the logarithmic length changes  $-\omega_{ij} = \log |z_{ij}| - \log |w_{ij}|$  of the edges. The dependent variables are the relative counterclockwise rotation angles  $\nu_{ij} = \arg(z_{ij}) - \arg(w_{ij})$  (modulo  $2\pi$ ) of the edges. For two incident edges in a triangle  $\Delta[z_i, z_j, z_k]$ , the differences  $\nu_{ki} - \nu_{jk}$  (modulo  $2\pi$ ) give the change of the angle  $\alpha_k^{\Delta[z_i, z_j, z_k]} - \alpha_k^{\Delta[v_i, v_j, v_k]}$  opposite to the edge  $ij$ . Thus condition (18) expresses in this case that the sum of opposite angles in the two incident triangles sharing an edge does not change. This encodes the usual condition for circle patterns that intersection angles are preserved.

Let  $\Phi_{ij}$  be the sums of opposite angles in two adjacent embedded triangles sharing the edge  $[v_i, v_j]$ . Recall that this is the exterior intersection angle between the corresponding circumcircles of the triangles. For a boundary edge we set  $\Phi_{ij}$  equal to the opposite angle. Then as detailed in [7, App. C], a corresponding concave functional is given by

$$\mathcal{F}_{\frac{\pi}{2}}(\omega) = - \sum_{\Delta[v_i, v_j, v_k]} \hat{V}(\log |w_{ij}| - \omega_{ij}, \log |w_{jk}| - \omega_{jk}, \log |w_{ki}| - \omega_{ki}) - \sum_{[v_i, v_j]} \Phi_{ij} \omega_{ij},$$

where the first sum is taken over all triangles and the second sum over all edges of the given triangulation  $T$ .

The function  $\hat{V}$  is defined for variable  $(\rho_{12}, \rho_{23}, \rho_{31}) \in \mathbb{R}^3$  such that the positive numbers  $\ell_{12} = e^{\rho_{12}}$ ,  $\ell_{23} = e^{\rho_{23}}$ ,  $\ell_{31} = e^{\rho_{31}}$  satisfy the triangle inequalities ( $\ell_{ij} + \ell_{jk} \geq \ell_{ki}$ ). In the

triangle with these edge lengths denote by  $\alpha_i^{jk}(\rho_{jk}, \rho_{ij}, \rho_{ki})$  the angle at vertex  $i$  opposite to the edge of lengths  $\ell_{jk} = e^{\rho_{jk}}$ . Then,

$$\begin{aligned} \hat{V}(\rho_{12}, \rho_{23}, \rho_{31}) &= \rho_{23} \alpha_1^{23}(\rho_{23}, \rho_{31}, \rho_{12}) + \rho_{31} \alpha_2^{31}(\rho_{31}, \rho_{12}, \rho_{23}) + \rho_{12} \alpha_3^{12}(\rho_{12}, \rho_{23}, \rho_{31}) \\ &\quad + 2\mathbb{J}(\alpha_1^{23}(\rho_{23}, \rho_{31}, \rho_{12})) + 2\mathbb{J}(\alpha_2^{31}(\rho_{31}, \rho_{12}, \rho_{23})) + 2\mathbb{J}(\alpha_3^{12}(\rho_{12}, \rho_{23}, \rho_{31})), \end{aligned} \quad (19)$$

where  $\mathbb{J}(x) = -\int_0^x \log |2 \sin(t)| dt$  is Milnor's Lobachevsky function.

According to the domain of definition of  $\hat{V}$ , the functional  $\mathcal{F}_{\frac{\pi}{2}}$  has to be considered on the domain

$$A = \{\omega \in \mathbb{R}^{|E|} \mid \text{for all edges } [v_i, v_j] \text{ and their incident triangles } \Delta[v_i, v_j, v_k] \text{ there holds } |w_{jk}|e^{-\omega_{jk}} + |w_{ki}|e^{-\omega_{ki}} \geq |w_{ij}|e^{-\omega_{ij}}\}.$$

Note that the functional  $\mathcal{F}_{\frac{\pi}{2}}$  may be extended from the domain  $A$  to  $\mathbb{R}^E$  such that the extension is still continuously differentiable and concave, see [7, Section 4.2].

**5.3.2. Conformally equivalent triangulations.** The case  $\vartheta = 0$  may be considered as ‘‘dual’’ to circle patterns. The free variables  $\omega_{ij}$  are the relative counterclockwise rotation angles  $\omega_{ij} = \arg(z_{ij}) - \arg(w_{ij})$  (modulo  $2\pi$ ) of the edges  $z_{ij}$ . The dependent variables  $\nu_{ij} = \log |z_{ij}| - \log |w_{ij}|$  are the changes of the logarithmic lengths of the edges. In this case, condition (18) expresses that the logarithm of the length cross-ratio does not change for any two incident triangles.

Denote by  $\alpha_i^{\Delta[z_i, z_j, z_k]} = \alpha_i^{\Delta[v_i, v_j, v_k]} + \omega_{ki} - \omega_{ij}$  the angle in the triangle  $\Delta[z_i, z_j, z_k]$  (with counterclockwise orientation) opposite to the edge  $z_{jk}$ . As detailed in [7, Sec. 4.3], a corresponding concave functional is given by

$$\begin{aligned} \mathcal{F}_0(\omega) &= \sum_{\Delta[v_i, v_j, v_k]} \left( 2\mathbb{J}(\alpha_i^{\Delta[v_i, v_j, v_k]} + \omega_{ki} - \omega_{ij}) + 2\mathbb{J}(\alpha_j^{\Delta[v_i, v_j, v_k]} + \omega_{ij} - \omega_{jk}) \right. \\ &\quad \left. + 2\mathbb{J}(\alpha_k^{\Delta[v_i, v_j, v_k]} + \omega_{jk} - \omega_{ki}) \right. \\ &\quad \left. + (\omega_{ki} - \omega_{ij}) \log |w_{jk}| + (\omega_{ij} - \omega_{jk}) \log |w_{ki}| + (\omega_{jk} - \omega_{ki}) \log |w_{ij}| \right). \end{aligned}$$

The variables have to be restricted to the domain

$$C = \{\omega \in \mathbb{R}^{|E|} \mid \text{for all vertices } v_i \text{ and their incident triangles } \Delta[v_i, v_j, v_k] : \alpha_i^{\Delta[v_i, v_j, v_k]} + \omega_{ki} - \omega_{ij} \in (0, \pi)\}.$$

**5.4. The functional  $\mathcal{F}_{\vartheta}(\omega)$  and its relations to discrete  $\vartheta$ -conformal maps.** Let  $F : T \rightarrow \hat{T}$  be a discrete immersion of a simply connected triangulation  $T$ . Following our reasoning in Subsection 5.1, we can define our new variables  $\omega$  on all edges  $E$  and obtain corresponding dependent variables  $\nu^{\Delta}(\omega)$  on the edges of the respective triangles  $\Delta$ . We assume that the variables  $\omega$  vary within a neighborhood of (given) values which give rise to a discrete  $\vartheta$ -conformal map. That is, we consider (small) perturbations of a discrete  $\vartheta$ -conformal map. In this way, we ensure that the  $\nu^{\Delta}(\omega)$ 's are well-defined and smooth.

We will show that condition (18) is variational. In particular, we consider the 1-form

$$\Xi_{\vartheta}(\omega) = \sum_{e=[v_i, v_j] \in E_{int}} (\nu_{il}^{\Delta_{ilj}} - \nu_{lj}^{\Delta_{ilj}} + \nu_{jk}^{\Delta_{ijk}} - \nu_{ki}^{\Delta_{ijk}}) d\omega_e, \quad (20)$$

where  $\omega \in \mathbb{R}^{|E|}$  denotes the vector of values of  $\omega_e$  on the edges and the sum is taken over all interior edges  $e = [v_i, v_j]$  which are contained in the two triangles  $\Delta_{ilj} = \Delta[v_i, v_l, v_j]$  and  $\Delta_{ijk} = \Delta[v_i, v_j, v_k]$  such that all edges in the triangles are enumerated in counterclockwise

orientation as in Figure 2(c). If the 1-form  $\Xi_\vartheta$  is closed, then we can locally integrate:  $\Xi_\vartheta = d\mathcal{F}_\vartheta$  where  $\mathcal{F}_\vartheta(\omega)$  is some function (defined on a suitable open subset). Furthermore, all critical points of  $\mathcal{F}_\vartheta$  satisfy (18) for all pairs of adjacent triangles.

**Theorem 5.3.** *The 1-form  $\Xi_\vartheta$  defined by (20) in a neighborhood of a solution is closed.*

*Proof.* By (20), the condition  $d\Xi_\vartheta = 0$  is equivalent to

$$\frac{\partial(v_{ij} - v_{jk})}{\partial\omega_{ij}} - \frac{\partial(v_{jk} - v_{ki})}{\partial\omega_{ki}} = 0$$

for every triangle  $\Delta[v_i, v_j, v_k]$  and cyclic permutations of the indices. Differentiating (16) by  $\omega_{ij}$  and  $\omega_{ki}$ , we see by straightforward calculations that

$$\begin{aligned} & \frac{\partial(v_{ij} - v_{jk})}{\partial\omega_{ij}} - \frac{\partial(v_{jk} - v_{ki})}{\partial\omega_{ki}} \\ &= \frac{\operatorname{Im}(w_{ij} \cdot ie^{i\vartheta} \cdot \exp(e^{i\vartheta}(i\omega_{ij} + (v_{ij} - v_{jk}))) \cdot \overline{w_{ki}} \cdot e^{-i\vartheta} \cdot \exp(e^{-i\vartheta}(-i\omega_{ki} + (v_{ki} - v_{jk}))))}{\operatorname{Im}(w_{ki} \cdot e^{i\vartheta} \cdot \exp(e^{i\vartheta}(i\omega_{ki} + (v_{ki} - v_{jk}))) \cdot \overline{w_{ij}} \cdot e^{-i\vartheta} \cdot \exp(e^{-i\vartheta}(-i\omega_{ij} + (v_{ij} - v_{jk}))))} \\ & \quad + \frac{\operatorname{Im}(w_{ij} \cdot e^{i\vartheta} \cdot \exp(e^{i\vartheta}(i\omega_{ij} + (v_{ij} - v_{jk}))) \cdot \overline{w_{ki}} \cdot (-i)e^{-i\vartheta} \cdot \exp(e^{-i\vartheta}(-i\omega_{ki} + (v_{ki} - v_{jk}))))}{\operatorname{Im}(w_{ki} \cdot e^{i\vartheta} \cdot \exp(e^{i\vartheta}(i\omega_{ki} + (v_{ki} - v_{jk}))) \cdot \overline{w_{ij}} \cdot e^{-i\vartheta} \cdot \exp(e^{-i\vartheta}(-i\omega_{ij} + (v_{ij} - v_{jk}))))} \\ &= \frac{\operatorname{Im}(w_{ij}\overline{w_{ki}}\exp(e^{i\vartheta}(i\omega_{ij} + (v_{ij} - v_{jk})) + e^{-i\vartheta}(i\omega_{ki} + (v_{ki} - v_{jk}))(ie^{i\vartheta} \cdot e^{-i\vartheta} - ie^{-i\vartheta} \cdot e^{i\vartheta}))}{\operatorname{Im}(w_{ki}\overline{w_{ij}}\exp(e^{i\vartheta}(i\omega_{ki} + (v_{ki} - v_{jk})) + e^{-i\vartheta}(-i\omega_{ij} + (v_{ij} - v_{jk}))))} \\ &= 0. \end{aligned}$$

This shows that the 1-form  $\Xi_\vartheta$  is closed.  $\square$

**Theorem 5.4.** *The function  $\mathcal{F}_\vartheta$  which is a local integral of  $\Xi_\vartheta$  is locally concave, that is, the second derivative is a negative semidefinite quadratic form. Its one-dimensional kernel is spanned by  $(1, 1, \dots, 1)$ .*

*Proof.* The calculations in the proof of Theorem 5.3 show in fact that  $\frac{\partial(v_{ij} - v_{jk})}{\partial\omega_{ij}} = \cot \alpha_i^{\tilde{\Delta}_{ijk}}$ , where  $\alpha_i^{\tilde{\Delta}_{ijk}}(\omega)$  is the (positively oriented) angle in the triangle  $\tilde{\Delta}_{ijk} = \Delta[z_i, z_j, z_k]$  corresponding to the given values of  $\omega$ . Furthermore, by similar calculations we obtain  $\frac{\partial(v_{ij} - v_{jk})}{\partial\omega_{ki}} = -\cot \alpha_k^{\tilde{\Delta}_{ijk}} - \cot \alpha_i^{\tilde{\Delta}_{ijk}}$ . This shows by the same arguments as in [7, Prop. 4.2.4], that the Hessian of the functional  $\mathcal{F}_\vartheta$  is a negative semidefinite quadratic form  $-\sum_{e \cong \tilde{e}} \cot \alpha^{e, \tilde{e}} (d\omega_e - d\omega_{\tilde{e}})^2$  where the sum is taken over all pairs of edges  $e, \tilde{e}$  which are incident to the same triangular face and  $\alpha^{e, \tilde{e}}$  is the angle between these edges. The one-dimensional kernel is spanned by  $(1, 1, \dots, 1)$ .  $\square$

It is interesting to note that the entries of the second derivative of  $\mathcal{F}_\vartheta$  (at  $\omega = 0$ ) are the same (up to sign) as in the known cases for circle patterns and discrete conformal equivalence, see for example [7].

We have now proved the first part of Theorem 5.1. In order to use the variational principle for computational purposes, it is important that maximizers  $\omega$  of  $\mathcal{F}_\vartheta$  also correspond to discrete  $\vartheta$ -conformal maps, which can be obtained from the values of  $\omega$  and  $v(\omega)$  by gluing the corresponding triangles according to the given combinatorics.

**Theorem 5.5.** *Every maximizer of  $\mathcal{F}_\vartheta$  on a simply connected triangulation gives rise to a  $\vartheta$ -conformal map.*

*Proof.* Note that we implicitly assume that every maximizer  $\omega$  lies in the “allowed domain”, that is, for every triangle there exist values for the depending parameters  $\nu$  to the corresponding values of  $\omega$ . So locally,  $\omega$  gives rise to a realization of triangles which is an orientation preserving embedding.

We prove the claim by successive construction of an immersed triangulation with the same combinatorics as the given one and such that (3) holds for all pairs of incident triangles. Start with any triangle and its realization, that is suitable values for  $\nu$  on the edges such that (16) holds. As the values of  $\nu$  are unique up to a common additive constant, this corresponds to fixing a similarity transformation.

Next we consider an incident triangle. We know by assumption, that suitable dependent parameters  $\nu$  exist on its edges and fix the freedom for  $\nu$  by choosing  $\nu_{ij}$  to agree with the value from the first triangle on the common edge  $[v_i, v_j]$ . This uniquely determines the remaining two values for  $\nu$  and thus the embedding of the second triangle. Note that by assumption the values of  $\nu$  on the boundary edges of the pair of incident triangles satisfy (18). We can successively continue this procedure and obtain further values for  $\nu$  and a sequence of embedded triangles according the given combinatorics as long as this sequence never closes up. In this case, there might appear two different values for  $\nu$  on the same edge (i.e. the corresponding triangles cannot be glued together).

By assumption, the given triangulation is simply connected. Therefore, it is sufficient to show that no ambiguities occur if we consider the sequence of incident triangles  $\Delta[v_0, v_j, v_{j+1}]$ ,  $j = 1, \dots, n$ ,  $n + 1 = 1$ , which build a flower. Assume without loss of generality that we start with  $\Delta[v_0, v_1, v_2]$  and given  $\nu$ 's on the edges and then successively determine the value of the  $\nu$ 's on the other edges. All these values are well-defined except possibly the value on the edge  $[v_0, v_1]$ . Here,  $\nu_{0,1}$  is initially given, but following our construction gives some value  $\nu_{0,1}^*$  in the triangle  $\Delta[v_0, v_n, v_1]$  which might be different. But we can sum up condition (18), which holds for all pairs of incident triangles, in particular

$$\begin{aligned} \nu_{0,j} - \nu_{j,j+1} + \nu_{j+1,j+2} - \nu_{0,j+2} &= 0 \quad \text{for } j = 1, \dots, n-2, \\ \nu_{0,n-1} - \nu_{n-1,n} + \nu_{n,1} - \nu_{0,1}^* &= 0 \\ \nu_{0,n} - \nu_{n,1} + \nu_{1,2} - \nu_{0,2} &= 0. \end{aligned}$$

Adding up all these equations leads to  $\nu_{0,1} - \nu_{0,1}^* = 0$ . This proves that the values of  $\nu$  are well-defined on a flower.

Therefore, starting with any triangle, we can successively determine the values of  $\nu$  on all edges and thus successively embed all triangles. This gives a discrete immersion  $F$ . Condition (18) implies that  $F$  is also  $\vartheta$ -conformal.  $\square$

**5.5. A variational principle with variables at vertices.** For our variational principle explained above, we start from real parameters  $\omega_e$  on the *edges* of the triangles (which then determine  $\nu^\Delta(\omega)$  by (16) and finally lead to an immersed triangulation). Alternatively, one can consider real parameters  $u_i$  on the *vertices* of the triangles. This is similar to the logarithmic scale factors considered in [7] and Remark 3.6. To every edge  $[v_i, v_j]$  we then associate the arithmetic mean  $(u_i + u_j)/2$ . Denoting the dependent parameters by  $\xi = \xi(u)$ , we can reformulate (16) as

$$\begin{aligned} w_{ij} \cdot \exp(e^{i\vartheta}((u_i + u_j)/2 + i(\xi_i + \xi_j)/2)) + w_{jk} \cdot \exp(e^{-i\vartheta}((u_j + u_k)/2 + i(\xi_j + \xi_k)/2)) \\ + w_{ki} \cdot \exp(e^{-i\vartheta}((u_k + u_i)/2 + i(\xi_k + \xi_i)/2)) = 0. \end{aligned} \quad (21)$$

Analogously as for  $\nu(\omega)$ , these dependent values  $\xi(u)$  are only unique up to a common constant and depend on all values of  $u$  in the triangle  $\Delta[v_i, v_j, v_k]$ .

We will now reformulate the condition for discrete  $\vartheta$ -conformal maps in these variables. To this end, consider a flower as for example in Figure 2(b). Assume that values  $u_j$  are given on the center of the flower  $v_0$  and all its incident vertices  $v_1, \dots, v_N$  such that there exist a solution of (21) in every triangle. Similarly as in (15), the oriented angle between the edges  $[z_0, z_j]$  and  $[z_0, z_{j+1}]$  is

$$\alpha_{j,j+1}^{\Delta[z_0, v_j, v_{j+1}]} = \alpha_{j,j+1}^{\Delta[v_0, v_j, v_{j+1}]} + \frac{1}{2}(u_{j+1} - u_j) \sin \vartheta + \frac{1}{2}(\xi_{j+1}^{\Delta_{0,j,j+1}} - \xi_j^{\Delta_{0,j,j+1}}) \cos \vartheta.$$

Recall that the dependent parameters  $\xi_{j+1}^{\Delta_{0,j,j+1}} - \xi_j^{\Delta_{0,j,j+1}}$  are defined locally in the triangles  $\Delta_{0,j,j+1} = \Delta[v_0, v_j, v_{j+1}]$  at the vertex  $v_0$ . Note that  $\xi_{j+1}^{\Delta_{0,j,j+1}} - \xi_j^{\Delta_{0,j,j+1}}$  smoothly depends on the given values  $u_j, u_{j+1}, u_0$  in a neighborhood of a solution. Then this flower can only be embedded if the following closing condition holds:

$$0 = \sum_{j=1}^6 (e^{-i\vartheta}(u_{j+1} - u_j) + ie^{-i\vartheta}(\xi_{j+1}^{\Delta_{0,j,j+1}} - \xi_j^{\Delta_{0,j,j+1}})) = ie^{-i\vartheta} \sum_{j=1}^6 (\xi_{j+1}^{\Delta_{0,j,j+1}} - \xi_j^{\Delta_{0,j,j+1}}), \quad (22)$$

where we identify indices modulo 6. Condition (22) is variational, if for any two adjacent triangles  $\Delta[v_i, v_l, v_j]$  and  $\Delta[v_i, v_j, v_k]$  we have

$$\frac{\partial(\xi_k^{\Delta_{i,j,k}} - \xi_j^{\Delta_{i,j,k}})}{\partial u_j} + \frac{\partial(\xi_j^{\Delta_{i,l,j}} - \xi_l^{\Delta_{i,l,j}})}{\partial u_j} = \frac{\partial(\xi_i^{\Delta_{i,j,k}} - \xi_k^{\Delta_{i,j,k}})}{\partial u_i} + \frac{\partial(\xi_l^{\Delta_{i,l,j}} - \xi_i^{\Delta_{i,l,j}})}{\partial u_i}.$$

This in turn is true as straightforward calculations (for example using a computer algebra system) show that if  $\Delta_{1,2,3} = \Delta[v_1, v_2, v_3]$  is an embedded non-degenerate triangle with angles  $\alpha_1, \alpha_2, \alpha_3 \in (0, \pi)$  at the corresponding vertices, we have

$$\frac{\partial}{\partial u_3} (\xi_3^{\Delta_{1,2,3}} - \xi_2^{\Delta_{1,2,3}})/2 = \cot \alpha_2 = \frac{\partial}{\partial u_1} (\xi_2^{\Delta_{1,2,3}} - \xi_1^{\Delta_{1,2,3}})/2.$$

This also proves that the Hessian of the functional is again the cotan-Laplacian as it is the case for conformal equivalence and for circle patterns. Furthermore, this implies that the corresponding functional is locally concave and therefore the maximizers are unique (up to a global transformation).

Brief review on known cases. For the known case of conformally equivalent triangulations ( $\vartheta = 0$ ), the variables  $u_i$  are logarithmic scale factors and the dependent variables  $\xi_i$  correspond to relativ rotations. A corresponding concave functional is studied in [7, Section 4] and given by

$$\begin{aligned} \mathcal{E}_0(u) = & - \sum_{\Delta[v_i, v_j, v_k]} \left( \hat{V}(\log |w_{ij}| + (u_i + u_j)/2, \log |w_{jk}| + (u_j + u_k)/2, \log |w_{ki}| + (u_k + u_i)/2) \right. \\ & \left. - \pi(u_i + u_j + u_k)/2 - \frac{\pi}{2}(\log |w_{ij}| + \log |w_{jk}| + \log |w_{ki}| + u_i + u_j + u_k) \right) \\ & - \sum_{v_i} \Theta_i u_i / 2, \end{aligned}$$

where the first sum is taken over all triangles and the second sum over all vertices of the given triangulation  $T$ . Note that [7] investigates twice the negative of this functional (that is  $E_{T, \Theta, \lambda}(u) = -2\mathcal{E}_0(u)$ ). The function  $\hat{V}$  has been defined in (19). The numbers  $\Theta_i$  are the desired angles sums at vertices of the image triangulation, so  $\Theta_i = 2\pi$  in our case for all interior vertices  $v_i \in V_{int}$ . For boundary vertices we either fix  $\Theta_i$  or  $u_i$ , see [7, Section 3.1]. Note that the functional  $\mathcal{E}_0$  is only defined on a part of  $\mathbb{R}^{|V|}$ , namely where all triangle

inequalities for the new edge lengths (given by  $|w_{ij}|e^{(u_i+u_j)/2}$ ) hold. But this functional may be extended to a concave continuously differentiable functional on  $\mathbb{R}^{|V|}$ , see [7, Prop. 4.1.5].

For the known case of circle patterns ( $\vartheta = \pi/2$ ), the variables  $u_i$  are the relative counterclockwise rotation angles of the edge stars at  $v_i$  and the dependent variables  $\xi_i$  are logarithmic scale factors. A corresponding concave functional is studied in [9, Section 6.2] and given by

$$\mathcal{E}_{\frac{\pi}{2}}(u) = \sum_{\Delta[v_i, v_j]} (\mathcal{J}\mathcal{I}(\alpha_k^{\Delta[v_i, v_j, v_k]} + (u_j - u_i)/2) + \mathcal{J}\mathcal{I}(\alpha_l^{\Delta[v_i, v_l, v_j]} + (u_i - u_j)/2)),$$

where the sum is taken over all interior edges  $[v_i, v_j]$  of  $T$  with incident, counterclockwise oriented triangles  $\Delta[v_i, v_j, v_k]$  and  $\Delta[v_i, v_l, v_j]$ . Note that also this functional is not defined for all possible values of  $u \in \mathbb{R}^{|V|}$ , as we need all angles  $\alpha_k^{\Delta[v_i, v_j, v_k]} + (u_j - u_i)/2$  to only take values in  $(0, \pi)$ .

## 6. CONCLUDING REMARKS

Relations to Ronkin functions, amoebas and coamoebas. It is interesting to note that the functional  $\hat{V}$  defined in (19), which reappears in the formula for  $\mathcal{E}_0$ , is the Ronkin function of the linear polynomial  $z_1 + z_2 + z_3$ , see [7, Remark 4.2.7] and the references therein. The domain of definition of  $\hat{V}$  is an amoeba. This notion was introduced in [21] by Gelfand, Kapranov and Zelevinsky. The amoeba of a complex polynomial  $p(z_1, \dots, z_n)$  is defined as the image of the set of zeros of  $p$  under the map  $(z_1, \dots, z_n) \mapsto (\log |z_1|, \dots, \log |z_n|)$ . A coamoeba, also called Newton polygon or Newton polytope, constitutes a closely related “dual” notion, see for example [31] for a nice introductory presentation. Similarly as for amoeba and coamoeba, our considerations are based on logarithmic coordinates. Unfortunately, it is still unclear why the Ronkin function is related to some of the known functionals and how to connect the known explicit formulas for the functionals detailed in Section 5.3 into a common framework.

Relations to hyperbolic polyhedra and their duals. Recall that discretely conformally equivalent triangulations are described intrinsically via edge lengths. Furthermore, this approach is related to hyperbolic polyhedra, see [7, 38]. But it was also noted soon that the theory of discrete conformal equivalence requires changes in the combinatorics or else faces the degeneration of triangles (as indicated in the proofs of Lemma 3.8 and Lemma 4.1).

On the other hand, circle patterns are defined using intersection angles which are not intrinsic variables. If we stereographically project a circle pattern to the sphere and regard this sphere as the boundary of hyperbolic space, we can associate to every circle a hyperbolic plane. The interior intersection angles between intersecting circles agree with the dihedral angles between the corresponding intersecting hyperbolic planes. The ideal hyperbolic polyhedron which is bounded by these planes is determined by the dihedral angles between these planes. Instead, one can consider the dual polyhedron as defined by Rivin in [25, 33] using a suitable Gauss-map. Rivin then characterized this dual polyhedron via its metric.

It remains an open question how the one parameter family of discrete  $\vartheta$ -conformal maps may be related to a corresponding family of polyhedra which interpolates between the two known cases.

**Funding.** This work was supported by the DFG Collaborative Research Center TRR 109 “Discretization in Geometry and Dynamics”.

## ACKNOWLEDGMENTS

The author is grateful to Alexander Bobenko for initiating her research on conformally symmetric triangulations.

Furthermore, it is a pleasure to thank Boris Springborn, Wai Yeung Lam, and, in particular, Niklas Affolter for interesting discussions on discrete  $\vartheta$ -conformal maps and their connections to circle patterns and discrete conformal equivalence. Interesting insight into the variational principle for the discrete  $\vartheta$ -conformal maps has been gained during the inspiring Young Investigator’s Workshop of the DFG Collaborative Research Center TRR 109 “Discretization in Geometry and Dynamics” in March 2018.

This research was supported by the DFG Collaborative Research Center TRR 109 “Discretization in Geometry and Dynamics”.

## REFERENCES

1. Sergei I. Agafonov and Alexander I. Bobenko, *Discrete  $Z^2$  and Painlevé equations*, Internat. Math. Res. Notices **4** (2000), 165–193.
2. Alan F. Beardon, Tomasz Dubejko, and Kenneth Stephenson, *Spiral hexagonal circle packings in the plane*, Geom. Dedicata **49** (1994), 39–70.
3. Alexander I. Bobenko, *Discrete conformal maps and surfaces*, Symmetries and Integrability of Difference Equations (P. A. Clarkson and F. W. Nijhoff, eds.), London Mathematical Society Lecture Notes Series, vol. 255, Cambridge University Press, 1999, pp. 97–108.
4. Alexander I. Bobenko and Tim Hoffmann, *Conformally symmetric circle packings. a generalization of Doyle spirals*, Experiment. Math. **10** (2001), 141–150.
5. ———, *Hexagonal circle patterns and integrable systems: Patterns with constant angles*, Duke Math. J. **116** (2003), 525–566.
6. Alexander I. Bobenko, Christian Mercat, and Yuri B. Suris, *Linear and nonlinear theories of discrete analytic functions. Integrable structure and isomonodromic Green’s function*, J. Reine Angew. Math. **583** (2005), 117–161.
7. Alexander I. Bobenko, Ulrich Pinkall, and Boris A. Springborn, *Discrete conformal maps and ideal hyperbolic polyhedra*, Geom. Topol. **19** (2015), no. 4, 2155–2215.
8. Alexander I. Bobenko, Stefan Sechelmann, and Boris A. Springborn, *Discrete conformal maps: Boundary value problems, circle domains, fuchsian and schottky uniformization*, pp. 1–56, Springer Berlin Heidelberg, 2016.
9. Alexander I. Bobenko and Boris A. Springborn, *Variational principles for circle patterns and Koebe’s theorem*, Trans. Amer. Math. Soc. **356** (2004), 659–689.
10. Alexander I. Bobenko and Yuri B. Suris, *Discrete differential geometry. Integrable structure*, Graduate Studies in Mathematics, vol. 98, AMS, 2008.
11. Ulrike Bücking, *Approximation of conformal mappings by circle patterns*, Geom. Dedicata **137** (2008), 163–197.
12. ———, *Introduction to linear and nonlinear integrable theories in discrete complex analysis*, Symmetries and Integrability of Difference Equations (D. Levi, R. Rebelo, and P. Winternitz, eds.), CRM Series in Mathematical Physics, Springer, 2017, pp. 153–193.
13. ———,  *$C^\infty$ -convergence of conformal mappings for conformally equivalent triangular lattices*, Results in Math. **73** (2018), no. 2.
14. Mauro Carfora and Annalisa Marzuoli, *Quantum triangulations. moduli spaces, quantum computing, non-linear sigma models and Ricci flow*, vol. 942, 2017.
15. Dmitry Chelkak and Stanislav Smirnov, *Discrete complex analysis on isoradial graphs*, Adv. Math. **228** (2011), no. 3, 1590–1630.
16. ———, *Universality in the 2D Ising model and conformal invariance of fermionic observables*, Invent. Math. **189** (2012), no. 3, 515–580.
17. Philippe G. Ciarlet, *The finite element method for elliptic problems*, Studies in mathematics and its applications, North-Holland, Amsterdam, 1978.
18. Yves Colin de Verdière, *Un principe variationnel pour les empilements de cercles*, Invent. Math. **104** (1991), no. 3, 655–669.
19. Nadav Dym, Raz Slutsky, and Yaron Lipman, *A linear variational principle for Riemann mappings and discrete conformality*, Proc. Natl. Acad. Sci. USA (PNAS) **116** (2019), no. 3.

20. Jacqueline Ferrand, *Fonctions préharmoniques et fonctions préholomorphes*, Bull. Sci. Math. **68** (1944), 152–180.
21. Israel M. Gelfand, Mikhail M. Kapranov, and Andrei V. Zelevinsky, *Discriminants, resultants, and multidimensional determinants.*, Boston, MA: Birkhäuser, 1994.
22. J. D. Gergonne, *Questions proposées/résolues*, Ann. Math. Pure Appl. **7** (1816), 68, 99–100, 156, 143–147.
23. David Glickenstein, *Discrete conformal variations and scalar curvature on piecewise flat two- and three-dimensional manifolds*, J. Differential Geom. **87** (2011), no. 2, 201–237.
24. Xianfeng Gu, Ren Guo, Feng Luo, Jian Sun, and Tianqi Wu, *A discrete uniformization theorem for polyhedral surfaces ii*, J. Differential Geom. **109** (2018), no. 3, 431–466.
25. Craig D. Hodgson and Igor Rivin, *A characterization of compact convex polyhedra in hyperbolic 3-space.*, Invent. Math. **111** (1993), no. 1, 77–111.
26. Richard Kenyon, *The Laplacian and Dirac operators on critical planar graphs*, Invent. math. **150** (2002), 409–439.
27. Liliya Kharevych, Boris A. Springborn, and Peter Schröder, *Discrete conformal mappings via circle patterns*, ACM Trans. Graph. **25** (2006), 412–438.
28. Wai Yeung Lam, *Discrete minimal surfaces: Critical points of the area functional from integrable systems*, International Mathematics Research Notices **2018** (2018), no. 6, 1808–1845.
29. Wai Yeung Lam and Ulrich Pinkall, *Holomorphic vector fields and quadratic differentials on planar triangular meshes*, pp. 241–265, Springer Berlin Heidelberg, 2016.
30. Feng Luo, *Combinatorial Yamabe flow on surfaces*, Commun. Contemp. Math. **6** (2004), no. 5, 765–780.
31. Mikael Passare, *How to computer  $\sum 1/n^2$  by solving triangles*, The American Mathematical Monthly **115** (2008), no. 8, 745–752.
32. Igor Rivin, *Euclidean structures on simplicial surfaces and hyperbolic volume*, Ann. of Math. **139** (1994), 553–580.
33. Igor Rivin, *A characterization of ideal polyhedra in hyperbolic 3-space.*, Ann. Math. (2) **143** (1996), no. 1, 51–70.
34. Oded Schramm, *Circle patterns with the combinatorics of the square grid*, Duke Math. J. **86** (1997), 347–389.
35. Mikhail Skopenkov, *The boundary value problem for discrete analytic functions*, Adv. Math. **240** (2013), 61–87.
36. Stanislav Smirnov, *Discrete complex analysis and probability*, Proceedings of the International Congress of Mathematicians. Volume I, Hindustan Book Agency, New Delhi, 2010, pp. 595–621.
37. Jerome Spanier and Keith B Oldham, *An atlas of functions*, Washington : Hemisphere Pub. Corp, 1987.
38. Boris A. Springborn, *Hyperbolic polyhedra and discrete uniformization*, e-print arXiv:1707.06848 [math.MG], 2017, To appear in Discrete Comput. Geom.
39. Boris A. Springborn, Peter Schröder, and Ulrich Pinkall, *Conformal equivalence of triangle meshes*, ACM Trans. Graph. **27** (2008), no. 3, 77:1–77:11.
40. William Thurston, *The finite Riemann mapping theorem*, Invited address at the International Symposium in Celebration of the proof of the Bieberbach Conjecture, Purdue University, 1985.
41. Tianqi Wu, Xianfeng Gu, and Jian Sun, *Rigidity of infinite hexagonal triangulation of the plane*, Trans. Amer. Math. Soc. **367** (2015), 6539–6555.